University Mohamed Khider of Biskra
Faculty of exact sciences
Matter sciences department

MASTER'S GRADUATION THESIS

Domain: Matter Sciences
Spinneret: Chemistry

Field: Pharmaceutical Chemistry
Ref:

Presented by: LAIB Maroua
Defended on: 03/06/2025

Green Synthesis, Characterization and Photocatalytic dye Degradation Activity of ZnO Nanoparticles

---

Jury:

Dr.	DJOUDI Linda	MCA	University Med Khider of Biskra	President
Dr.	LARAOUI Habiba	MCA	University Med Khider of Biskra	Supervisor
Dr.	MAANANI Djamila	MCB	University Med Khider of Biskra	Examiner

2024/2025


بسم الله الرحمن الرحيم

ACKNOWLWDGEMENT

By the name of Allah, the most merciful, the most compassionate all praise be to Allah, the lord of the worlds; and prayers and peace be upon Mohammed, his servant and messenger.

I would like to express my sincere gratitude to my supervisor, **Dr. LARAOUI Habiba**, for her guidance, encouragement, and invaluable advice throughout the course of this work. I am truly grateful for her mentorship and support.

I am deeply appreciative of the discussion committee members, **Dr. DJOUDI Linda** and **Dr. MAANANI Djamila**, for accepting to evaluate my work and for generously dedicating their time and expertise. Their constructive comments and feedback have been invaluable.

Special thanks go to **Dr. ACHOUR Achouak** for her support and assistance.

I am also grateful to all the members of the chemistry laboratory under the supervision of **Mrs. BENMACHICH Hayat** for their help and encouragement during my research.

I would like to express my heartfelt thanks to my family for their unwavering support and help.

Finally, I would like to thank everyone who assisted me throughout this study.

Marouа

DEDICATION

I would dedicate my effort to:

My angel in life, to the meaning of love and compassion who taught me the meaning of life and their existence is the reason for my success, who taught me to trust in Allah, believes in hard work and that so much could be done with little.

My parents

To the companion of the path and the support of life, thank you for your support and your presence by my side in situations the most difficult

To my fiance

My strength, who gave me love, cooperation and support me.

My brother and sisters

To my esteemed professors, whose guidance and inspiration have enriched my knowledge and skills

To all colleagues

To all family members young and old

CONTENTS

CHAPTER III: MATERIALS AND METHODS

CHAPTER IV: RESULTS AND DISCUSSION

ABBREVIATIONS

Symbol	Explanation
ZnO	Zinc oxide
NM	Nanomaterials
NPs	Nanoparticles
UV-vis	Ultra-Violet Visible Spectroscopy
FTIR	Fourier Transform Infra-Red Spectroscope
XRD	X-ray Diffraction Spectroscopy
rpm	Rotation per minute
KBr	Potassium Bromide
Min	Minutes
NaOH	Sodium Hydroxide
eV	Electron-Volt

LIST OF FIGURES

LIST OF TABLES

INTRODUCTION

Votre texte de paragraphe

INTRODUCTION

Over the years, there has been a marked increase in global interest toward sustainable and eco-friendly methods for synthesizing nanoparticles. Green synthesis, which emphasizes the use of non-toxic materials and eco-conscious processes, has become increasingly popular as a safer alternative to conventional chemical approaches. This approach offers a practical solution by employing bio-based materials such as microorganisms, plants, and agricultural waste as environmentally friendly sources for nanoparticle synthesis. One such approach that has gained significant interest in the scientific community is green synthesis using plant materials. Its attractiveness stems from its simplicity, environmental friendliness, and cost-effectiveness. Moreover, plant-mediated nano-synthesis produces biocompatible nanoparticles that can be employed for a wide range of applications [1].

Therefore, it is a viable alternative to chemical and physical nano-synthesis methods such as pulsed laser deposition, infrared irradiation, sputtering, chemical vapour deposition, etc. Even though some of these conventional nano-synthesis methods are widely used, they face drawbacks which include the use of hazardous chemicals, the need for pressure and temperature control, high energy consumption, high cost, and time constraints, all of which negatively impact the environment [2]. In contrast, green synthesis offers significant advantages; for instance, it enables a 30% decrease in energy usage, reduces costs by as much as 40%, and boosts production output by 50% compared to conventional synthesis methods [1].

Plant-mediated ZnO nanoparticles (NPs) have been extensively studied owing to their remarkable performance in a wide range of applications, including energy production and storage, medicine, environmental remediation, agriculture and food. Plants, for example, *Pluchea indica*, *Cnidoscolus aconitifolius*, *Mucuna pruriens*, *Scoparia Dulcis*, *Tilia Tomentosa*, *Azadirachta indica* (A. indica), *Zingiber Officinale* (Z. officinale) etc., has been successfully employed to produce ZnO NPs for a diverse array of applications, such as antibacterial, anticancer, antioxidant supercapacitors, photodegradation of dyes, agriculture, gas sensing, glucose sensing, solar cells, and sunscreens. Among these various applications, the photocatalytic degradation of dyes and antibacterial uses are the most extensively explored. This widespread attention is attributed to the

exceptional performance of plant-mediated ZnO NPs, which has been thoroughly documented in the scientific literature [3, 4].

Dyes are colored organic compounds widely employed across industries such as textiles, pharmaceuticals, food processing, tanneries, leather production, and cosmetics. However, their extensive use contributes significantly to industrial wastewater, as large quantities of these compounds are discharged during manufacturing processes. While conventional wastewater treatment technologies are commonly utilized, a major drawback of some of these methods is their inability to adequately treat dye-contaminated wastewater [5]. This inefficiency in conventional treatment methods raises urgent environmental and public health concerns, as discharging untreated or inadequately treated dye effluents into waterbodies poses a serious threat to human lives, aquatic ecosystems, and the environment. Photodegradation of dyes using semiconductor metal oxides such as ZnO NPs offers an alternative remedy that is consistent, secure, and capable of degrading dyes even at low concentrations [3, 6].

In this context, our study focuses on evaluating the photocatalytic activity of zinc oxide nanoparticles (ZnO NPs) through the degradation of Rhodamine B dye in aqueous solutions under sun light irradiation. The ZnO NPs are synthesized using medicinal Algerian plants from diverse botanical families, selected for their rich polyphenolic secondary metabolites. These metabolites are critical for reducing zinc precursors such as $ZnCl_2$ and stabilizing the resulting ZnO NPs. This work is divided into four chapters, starting from an introduction following by the first chapter that describe a comprehensive review of nanoparticles, including their classification, distinctive physicochemical characteristics and several synthesis methods, especially green synthesis. Additionally, the plants that have been selected for nanoparticle biosynthesis such as *Urtica dioica* (Stinging Nettle), *Atriplex halimus* (Saltbush), and *Equisetum arvense* (Horsetail) are also discussed in this chapter. The second chapter presents generalities on zinc oxide nanoparticles, their fields of applications, particular properties, green synthesis method and their characterization by using UV-Visible, XRD and FTIR techniques. The third chapter outlines the experimental procedures for ZnO NP biosynthesis, including extract preparation, reaction optimization (pH, temperature), and characterization workflows. The final chapter presents the results of the study. Finally, this work concludes with a summary of the main findings.

References

[1] Osman, A.I.; Zhang, Y.; Farghali, M.; Rashwan, A.K.; Eltaweil, A.S.; Abd El-Monaem, E.M.; Mohamed, I.M.A.; Badr, M.M.; Ihara, I.; Rooney, D.W.; et al. Synthesis of Green Nanoparticles for Energy, Biomedical, Environmental, Agricultural, and Food Applications: A Review. Environ. Chem. Lett. 2024, 22, 841–887. https://doi.org/10.1007/s10311-023-01682-3

[2] Prasad, A.R.; Williams, L.; Garvasis, J.; Shamsheera, K.O.; Basheer, S.M.; Kuruvilla, M.; Joseph, A. Applications of Phytogenic ZnO Nanoparticles: A Review on Recent Advancements. J. Mol. Liq. 2021, 331, 115805. https://doi.org/10.1016/j.molliq.2021.115805

[3] Tanwar, N.; Dhiman, V.; Kumar, S.; Kondal, N. Plant Extract Mediated ZnO-NPs as Photocatalyst for Dye Degradation: An Overview. Mater. Today Proc. 2021, 48, 1401–1406.

[4] Kavitha, A.; Doss, A.; Praveen Pole, R.P.; Pushpa Rani, T.P.K.; Prasad, R.; Satheesh, S. A Mini Review on Plant-Mediated Zinc Oxide Nanoparticles and Their Antibacterial Potency. Biocatal. Agric. Biotechnol. 2023, 48, 102654.

[5] Vidya, C.; Prabha, M.N.C.; Raj, M.A.L.A. Green Mediated Synthesis of Zinc Oxide Nanoparticles for the Photocatalytic Degradation of Rose Bengal Dye. Environ. Nanotechnol. Monit. Manag. 2016, 6, 134–138. https://doi.org/10.1016/j.enmm.2016.09.004

[6] Waseem, S.; Sittar, T.; Kayani, Z.N.; Gillani, S.S.A.; Rafique, M.; Asif Nawaz, M.; Masood Shaheen, S.; Assiri, M.A. Plant Mediated Green Synthesis of Zinc Oxide Nanoparticles Using *Citrus Jambhiri* Lushi Leaves Extract for Photodegradation of Methylene Blue Dye. Phys. B Condens. Matter 2023, 663, 415005.

CHAPTER I

LITERATURE REVIEW

I.1.Nanoscience and Nanotechnology

I.1.1. Definition of Nanoscience and Nanotechnology

The prefix 'nano' originates from Greek, signifying 'dwarf' or something exceedingly little, and represents one billionth of a meter (10^{-9} m). We should distinguish between nanoscience, and nanotechnology. Nanoscience is the study of structures and molecules on the scales of nanometers namely between 1 and 100 nm, and the technology that employs it in practical applications such as devices etc. is referred to as nanotechnology [1]. For comparison, a single human hair is about 60,000 nanometers thick, while the DNA double helix has a radius of approximately 1 nanometer (**Figure I.1**) [2]. The development and the use of nanomaterials in human objects and paraphernalia can be traced back to ancient times. In ancient Egypt, the soot of oil lamps was used to make black pigments for writing on papyrus. Around the time of 2575 BC, the Egyptians were already producing the synthetic pigment Egyptian blue. During the 5th century BC, the Greek philosopher Democritus, who is credited with formulating an atomic theory of the universe, investigated whether matter was a continuous substance that could be divided infinitely or if it was instead composed of fundamental, indivisible particles called *atomos*. He reasoned that the process of dividing matter must eventually end, resulting in tiny bodies with size and shape that could not be broken down further [3].

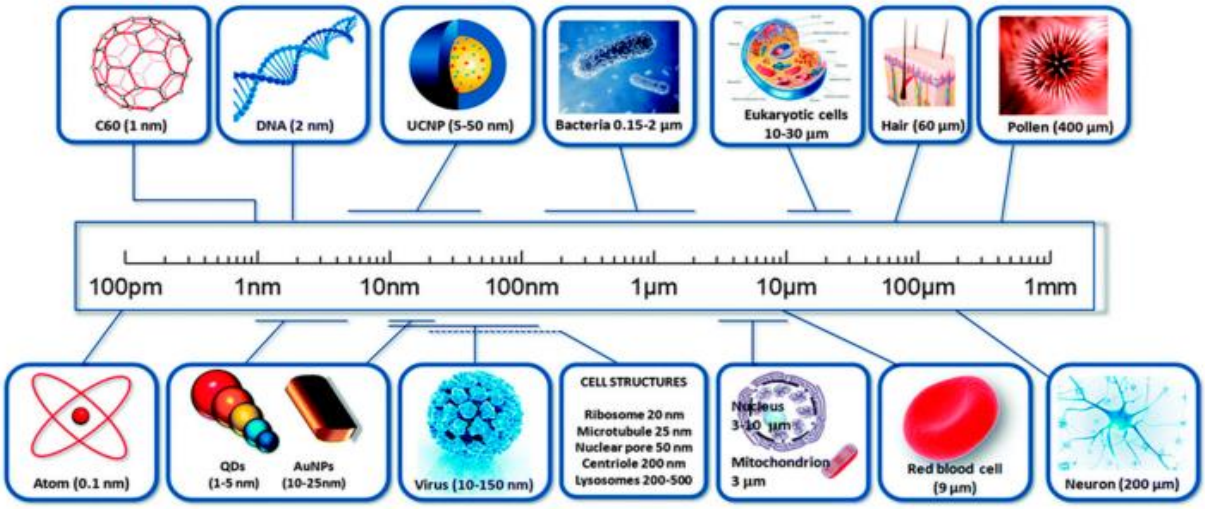

Figure I.1. Visualizing nanomaterial dimensions [2]

Nanotechnology, a key advancement of the 21st century, transforms nanoscience theories into practical applications by manipulating and controlling matter at the nanometer scale. The U.S. National Nanotechnology Initiative defines it as the science, engineering, and technology conducted at the nanoscale, enabling groundbreaking innovations across disciplines such as chemistry, biology, medicine, engineering, and electronics [4]. This definition highlights that nanotechnology involves manipulating structures at the nanometer level, controlling shape and size, and utilizing unique properties that emerge specifically at the nanoscale [5].

I.1.2. History of Nanotechnology

Nanoparticles and nanostructures have been utilized by humans as far back as the 4th century AD, exemplified by the Romans' innovative use of nanotechnology.

A remarkable example is the Lycurgus Cup, housed in the British Museum, which represents a significant achievement in ancient glassmaking. This artifact is the oldest known example of dichroic glass, a material that changes color under different lighting conditions. The cup appears green in direct light but shifts to red-purple when light passes through it (**Figure I.2**) [6]. This striking color change is not merely decorative but results from advanced material engineering far ahead of its time.

Figure I.2. The Lycurgus Cup’s Dichroic Effect: The glass appears green in reflected light (A) and red-purple in transmitted light (B) [6]

In 1857, Michael Faraday investigated "Ruby" gold colloids, demonstrating their distinctive optical properties and their ability to produce color variations under different lighting conditions [7]. The advancements in nanotechnology, made possible by breakthroughs in nanoscience, are summarized in Figure I.3.

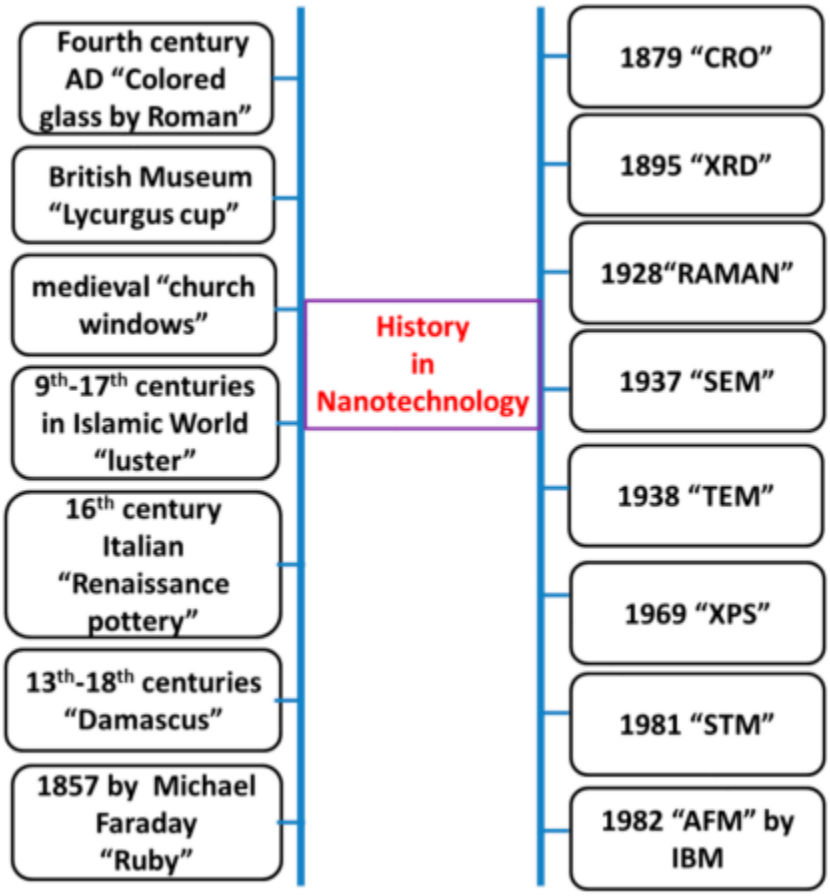

Figure I.3. Progresses in Nanotechnology

I.2.Nanomaterials

I.2.1. Definition

According to the International Organization for Standardization, the prefix "nano" refers to a size ranging approximately from 1 to 100 nm. As a comparison, the diameter of a carbon atom is about 0.25 nm, and the distance between carbon atoms is 0.15 nm. Nanomaterials are thus larger than single atoms or even small groups of atoms. Nature's examples of nano-sized objects include DNA molecules, which have a diameter of 25 nm, viruses, with the smallest identified one, parvovirus, being 25 nm wide, and proteins that are typically 10 nm long (**Figure I.4**) [8].

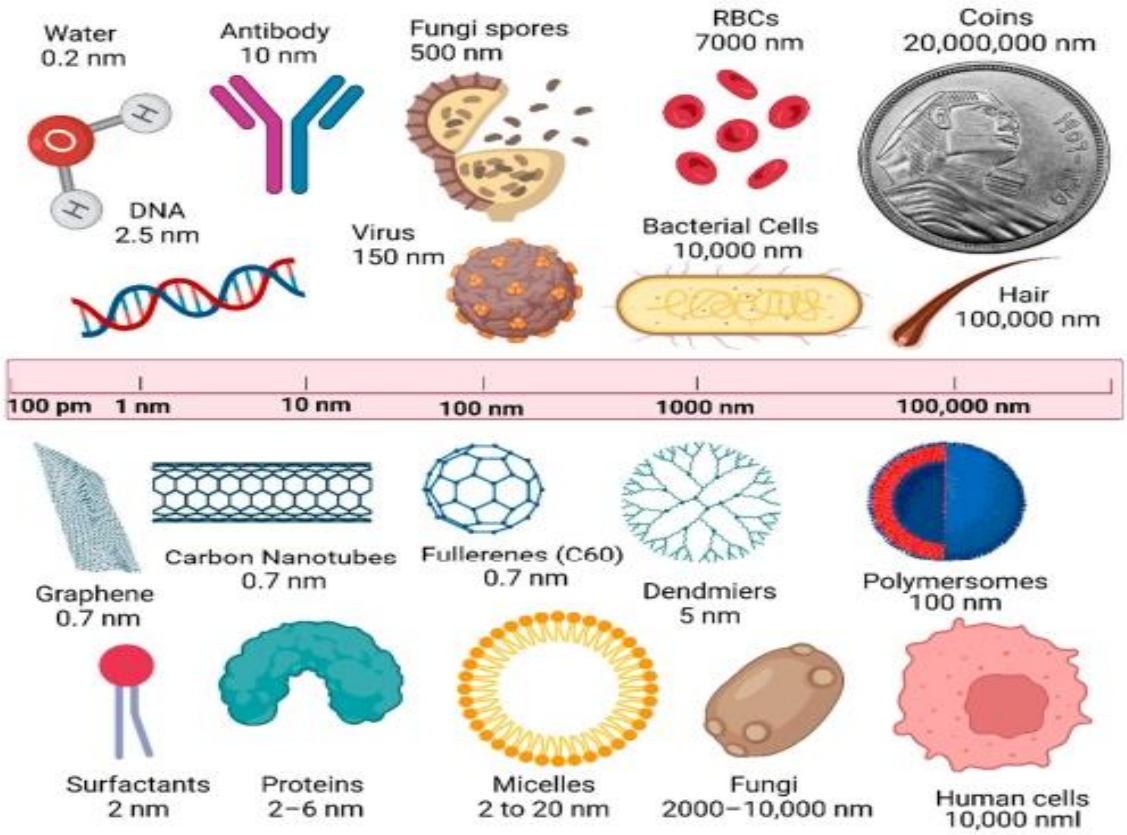

Figure I.4. Scheme showing the size scale of objects compared with the nanoscale size regime [8].

I.2.2. Classification of nanomaterials

Nanomaterials are classified into five distinct categories based on their size, origin, structural configuration, pore size, and potential toxicity, as illustrated in Figure bellow (**Figure I.5**) [9].

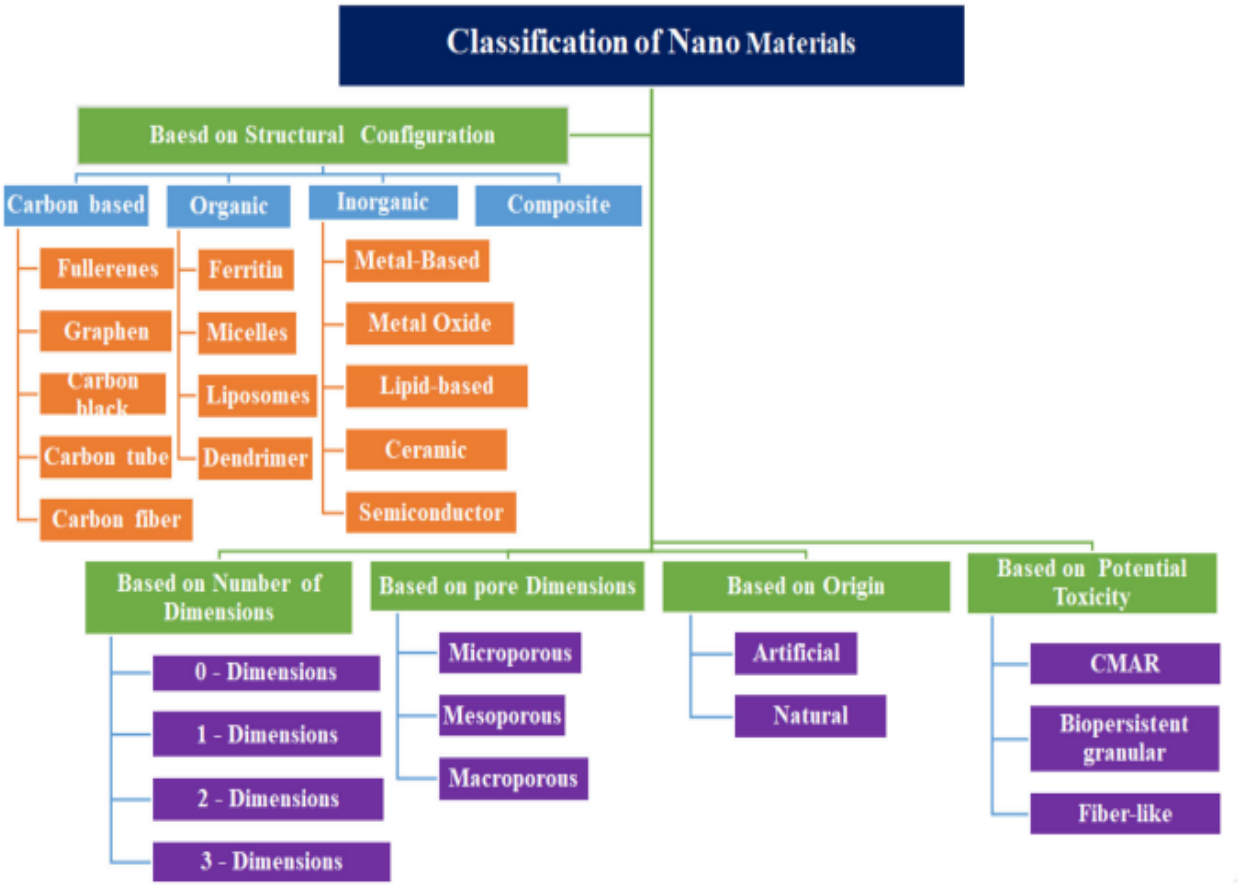

Figure I.5. General classification of nanomaterials

I.2.3. Properties of nanomaterials

The properties of nanometer-scale materials differ significantly from those of atoms and bulk materials due to surface charge/interaction, crystallography, composition, surface area, and nanoscale size effects, which can be seen in the magnetic, optical, electrical, mechanical, and chemical properties of nanomaterials [10,11].

I.2.3.1. Magnetic properties of nanomaterials

At the nanoscale, the magnetic behavior of materials changes due to the size of magnetic nanoparticles. Nanostructuring bulk magnetic materials improves properties, creating soft or hard magnets, increasing coactivity, and enabling super-paramagnetic behavior at critical grain sizes. Non-magnetic bulk materials, like gold and platinum, can exhibit magnetism at the nanoscale [12].

I.2.3.2. Optical properties of nanomaterials

Localized surface plasmon resonance (LSPR) is an optical property of nanoparticles. Some studies have shown that the line width is influenced by the size of nanoparticles. For example, by decreasing the size of Au nanoparticles, the emission light position changes from the Near-infrared to the ultraviolet (UV) region. At very small sizes, nanoparticles may lose their LSPR and become photoluminescent [13]. As a result of quantum confinement in nanomaterials, visible light emission can be tuned by varying the nanoscale dimensions. It has been discovered that as the size of the nanomaterials decreases, the peak emission shifts toward shorter wavelengths. Matter can change color at the nanoscale; for example, gold nanospheres can turn to yellow at 100 nm, greenish yellow at 50 nm, and red at 25 nm, while silver can also turn orange at 200 nm, light blue at 90 nm, and blue at 40 nm spherical thin film length [14, 15].

I.2.3.3 Electrical properties of nanomaterials

Nanomaterials change conductivity based on their scale and structure, increasing it in ceramics but raising resistance in metals due to quantum effects. Electron delocalization at nanoscale leads to discrete energy states, transforming metals into semiconductors like carbon nanotubes.

I.2.3.4. Chemical properties of nanomaterials

A substance’s applications are dictated by its chemical properties, such as reactivity, stability, flammability, corrosion resistance, oxidative potential, and reduction potential [16]. Nanomaterials, in particular, exhibit enhanced catalytic performance including superior reactivity, selectivity, and catalytic activity compared to their bulk material counterparts [12].

I.2.3.5. Mechanical properties

Mechanical properties, such as elasticity, ductility, tensile strength, and flexibility, are crucial for materials' applications. Nanomaterials have increased hardness, yield strength, elastic modulus, and toughness compared to bulk materials [17]. This increase is due to reduced defects and imperfection, improving alloy hardness, toughness, and super plasticity in ceramic [18–20].

I.2.4. Synthesis methods of nanomaterials

In general, nanomaterials are synthesized through various methods, which are classified into two main categories: bottom-up and top-down methods, as shown in **Figure I.6**.

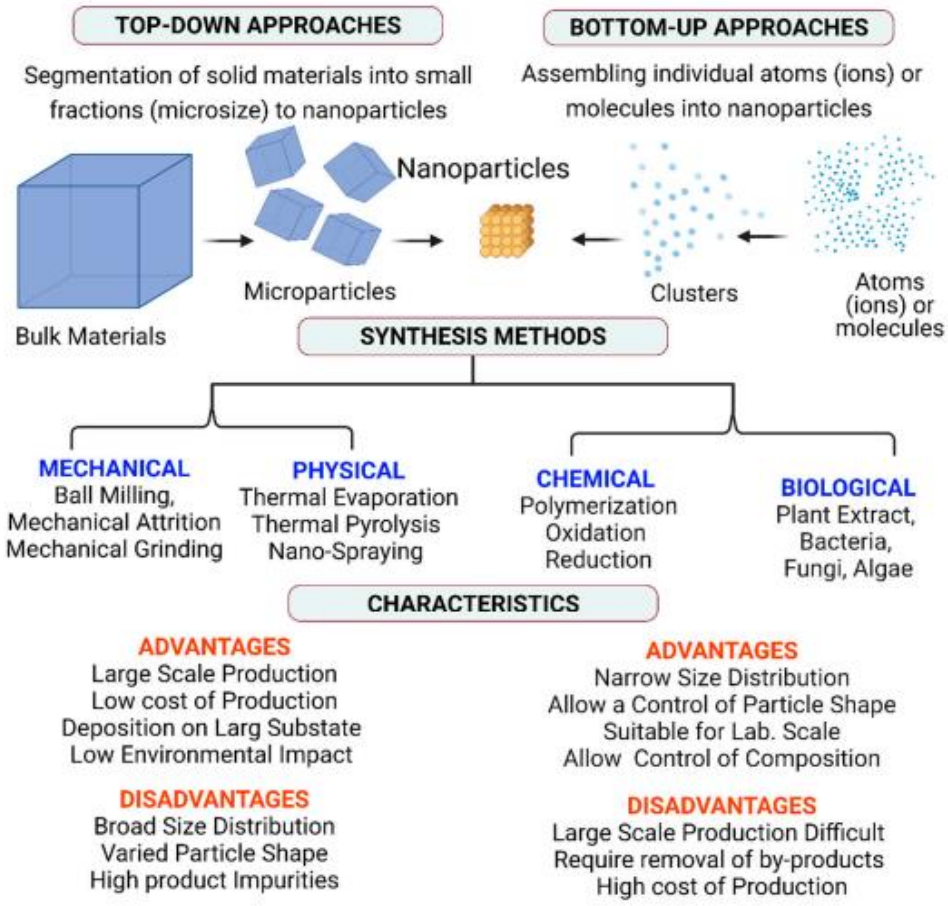

Figure I.6. Schematic presentation showing of the different fabrication techniques to produce nanomaterials and their advantages and disadvantages [7].

I.2.5. Applications of Nanomaterials

Nanomaterials have a wide range of general applications across various sectors due to their unique properties at the nanoscale. These include electronics and computing, medicine and healthcare, energy, environmental protection, materials science and engineering, textiles, and food as well as agriculture (**Figure I.7**) [21, 22, 23].

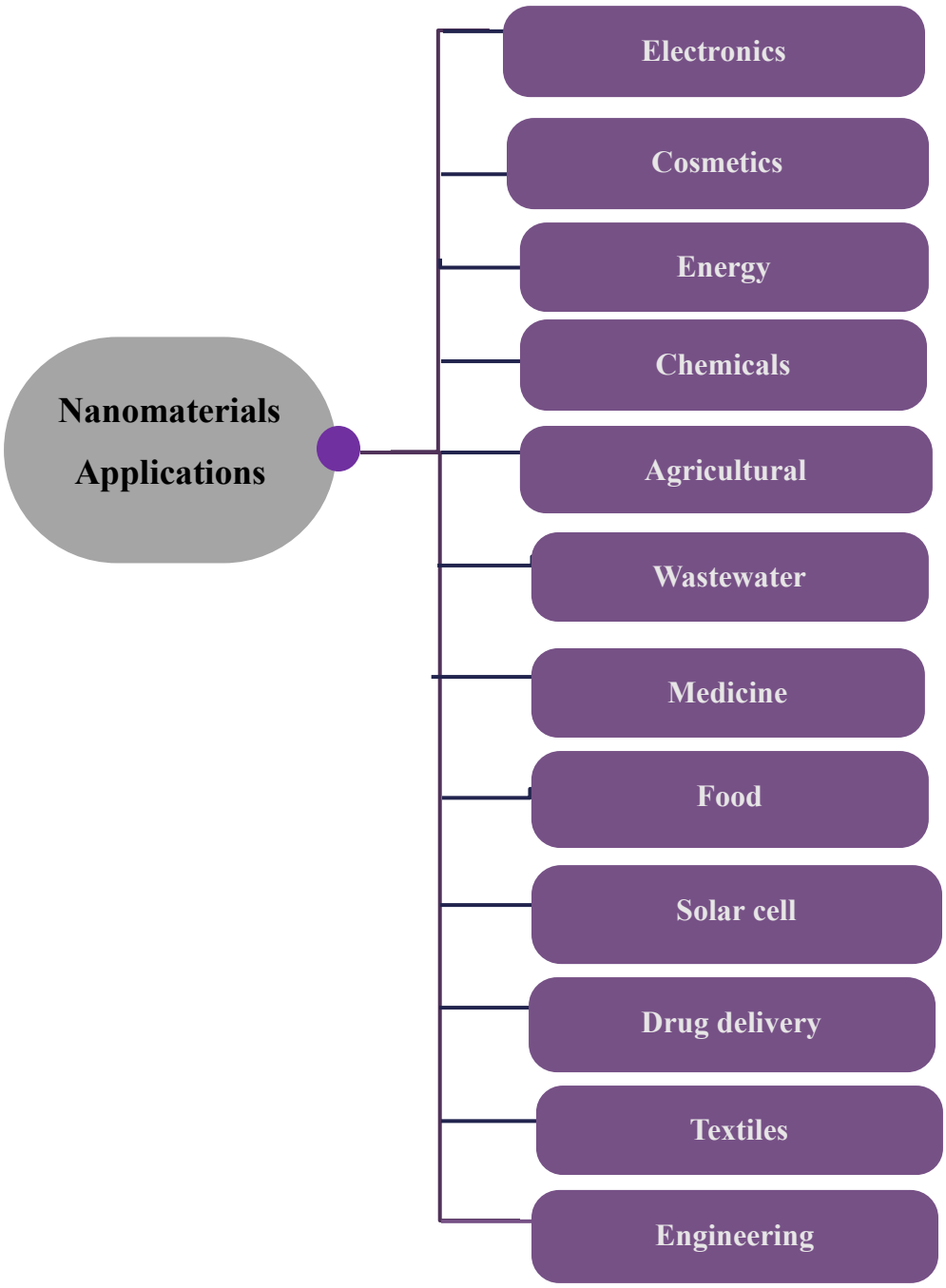

Figure I.7. Major Applications of Nanomaterials Across Key Sectors

I.2.6. Toxicity of Nanomaterials

The toxicity of nanomaterials can be influenced by a variety of physicochemical and biological factors, which determine how these materials interact with living systems and the environment. The following table (**Table I.6**) summarizes the key factors implicated in nanomaterial toxicity.

Table I.6. Factors implicated in nanomaterial toxicity

Factor	Nanomaterial Toxicity Effect	Ref
Dose and exposure duration	Nanoparticle's concentration in the medium multiplied by the exposure duration directly determines the number of nanoparticles in the body cells.	[24,25]
Aggregation and concentration	The toxicity of nanoparticles depends on their concentration; Higher nanoparticles concentrations favor their aggregation. aggregated nanoparticles may not easily enter cells, then their toxicity is decreased/abolished.	[26]
Nanoparticle size	Nanoparticles' size influences toxicity. For instance, cell penetration and toxicity are higher for small Ag NPs (~10 nm) than for Ag+ ions and larger Ag NPs (20–100 nm).	[27]
Nanoparticle morphology	Nanoparticle's toxicity varies in function of their aspect ratio. For instance, asbestos fibers of 10 μm in length may cause lung cancer, fibers between 5 and 10 μm may cause mesothelioma, and shorter fibers (2 μm) may cause asbestosis.	[28]
Surface area	Nanoparticle toxicity increases with smaller size and larger surface area, and their effects on human cells vary with the same mass dose of nanoparticles and microparticles.	[26]
Crystal structure	Nanoparticles' crystal structure influences the cellular uptake, oxidative mechanisms, and subcellular localization. For instance, the two TiO2 NPs polymorphs (rutile and anatase crystal structures) display different toxic effects. In the dark, rutile TiO2 NPs cause DNA damage by oxidation and this manages not caused by anatase nanoparticles.	[29]
Pre-exposure	Cell phagocytic activity can be enhanced by shorter exposure times or pre-exposure to nanoparticles at lower doses, allowing the human body to adapt to the nanoparticle.	[30]

I.3. Overview of the selected plants

I.3.1. *Urtica dioica* species

I.3.1.1. Description of the plant

Stinging nettle *(Urtica dioica L.*) (**Figure I.8**) is a common wild vegetable with a long history of use, this perennial herb is found almost globally, with a higher presence in Europe, North America, North Africa, and some regions of Asia [31, 32]. The plant is known for its stinging hairs that release chemicals causing irritation when touched [33]. In addition to its therapeutic and environmental significance, it generally attains heights of 1–2 meters and is characterized by its dark green, serrated, heart-shaped leaves adorned with stinging trichomes [34, 35]. The plant is dioecious, possessing male and female flowers on distinct specimens that flower from late spring to early autumn [36].

Figure I.8. Stinging nettle (photo taken by Tomislav Tosti)

I.3.1.2. Botanical classification of *Urtica dioica*

The following section provides a detailed overview of botanical classification of *U. dioica*:

- Kingdom: Plantae
- Subkingdom: Viridiplantae
- Superdivision: Embryophyta
- Division: Magnoliophyta
- Class: Magnoliopsida
- Family: Urticaceae
- Order: Rosales
- Arabic names; القريص, الحريق
- Genus: *Urtica*
- Species: *Urtica dioica*

I.3.1.3. Phytochemical composition of the plant

The phytochemical composition investigation on *U. dioica* demonstrated the presence of phenolic compounds (including flavonoids, tannins, coumarins and lignans), sterols, fatty acids, polysaccharides and isolectins [37–41].

Phenols and polyphenols in dietary plants garnered significant interest as therapeutic and prophylactic agents for chronic and degenerative diseases [38, 39]. It was noted that all components (roots, stem, and leaves) of *U. dioica* are abundant in these compounds, with larger concentrations found in wild specimens compared to domesticated ones. Root samples from Mediterranean cultivar were reported to contain phenol compounds, such ferulic acid and polyphenols as naringin, ellagic acid, myricetin and rutin (**Figure I.9**). The roots also included phytosterols (e.g., β-sitosterol), polysaccharides, isolectins, simple phenols (e.g., *p*-hydroxy-benzaldehyde), coumarins (e.g., scopoletin), triterpenoic acids and monoterpendiols [40].

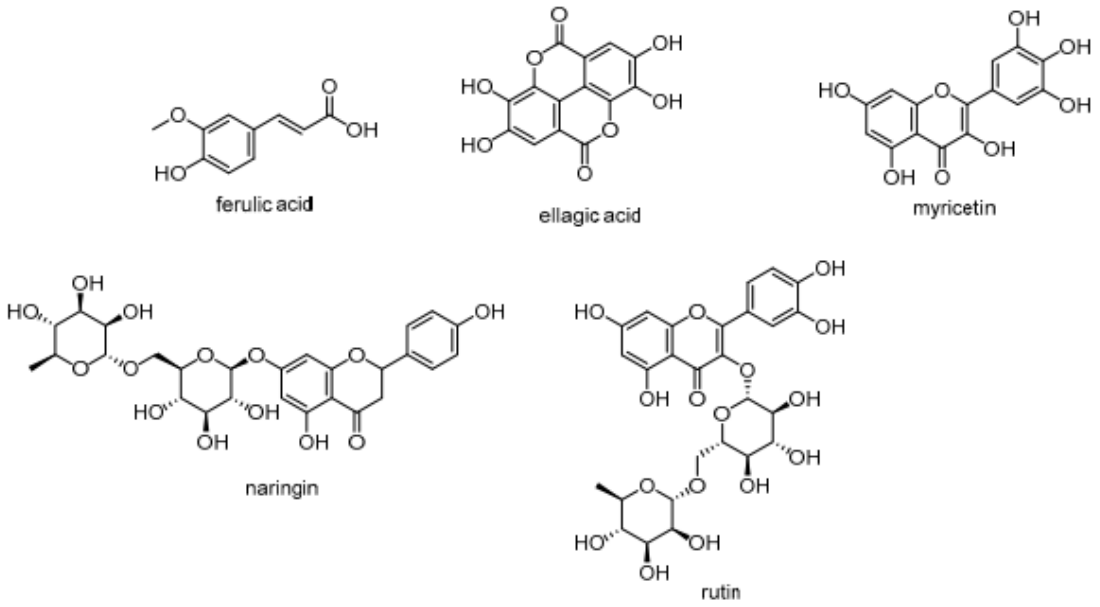

Figure I.9: Phenolic compounds from *U. dioica* [40]

I.3.1.4. Uses and Medicinal properties

The stinging nettle's extracts showed a variety of biological properties, including analgesic, antibacterial, anti-inflammatory, anti-ulcer, and antioxidant properties [41]. This plant is also used as a remedy for anemia, gout, eczema, and urinary, bladder, and a treatment for kidney issues [42]. It can also be commonly found in cosmetic preparations, and bast fibers can be used for the production of textiles [43, 44]. It is also part of many dishes such as soups, salads, and different food products like bread, cakes and chocolates, drinks and beverages, dairy products, and meat products [45]. Eventually, *U. dioica* is a source of chlorophyll, a food coloring ingredient (E140) used in the food and pharmaceutical industry [46].

I.3.1.5. Toxicity of the plant

Nettle (*Urtica dioica*) is commonly considered a harmless herb for cosmetic and medical uses, while its toxicity profile is dependent on the dosage. Research suggests that the plant exhibits low acute toxicity, with an LD_{50} exceeding 2,000 mg/kg in rats, implying no risk when used properly [47]. Nettle contains histamine and formic acid, which are responsible for its stinging sensation and may cause minor irritation or allergic reactions up on skin contact. These compounds are frequently removed during processing, making the plant safe for usage [48, 49].

I.3.2. *Atriplex halimus* species

I.3.2.1. Description of the plant

Atriplex halimus L. (**Figure I.10**) is an aromatic plant commonly known as "Rghel" and "Lgtef" [50]. *A. halimus* is a halophytic shrub that is widely distributed in arid and semi-arid Mediterranean areas, known for its tolerance to high salinity soils [51,52]. It is up to 3 meters tall, with the bark being grey-white in color and the leaves being 10–30 mm long and 5–20 mm wide. The leaves are a highly varied shape, ranging from deltoid-orbicular to lanceolate, with a short petiole at the base.

Figure I.10: *Atriplex halimus* plant

I.3.2.2. Botanical classification of *Atriplex halimus*

Atriplex halimus is classified botanically as follows:

- Kingdom: Plantae
- Division: Angiosperms
- Class: Magnoliopsida
- Order: Caryophyllales
- Family: Amaranthaceae
- Genus: *Atriplex*
- Species: *Atriplex halimus*
- Arabic names:**الأترج البحري, القطف**

I.3.2.3. Phytochemical composition of the plant

The bioactive components of *A. halimus* ethanolic extract (AHEE) were identified by an LC–MS/MS phytochemical analysis **(Figure I.11**). The results of this investigation revealed a high abundance of phenolic acids in the extract, with syringic acid, trans-ferulic acid, caffeic acid, and chlorogenic acid being the most prominent. Regarding flavonoid compounds, myricetin, catechin gallate (a flavan-3-ol), and trimethoxy flavone were detected in lower concentrations. Additionally, arbutin (a glycosylated hydroquinone) was identified in AHEE, though only in minimal amounts. Among all the phytoconstituents present in AHEE, gallic acid was the most abundant, followed by syringic acid and trans-ferulic acid [53].

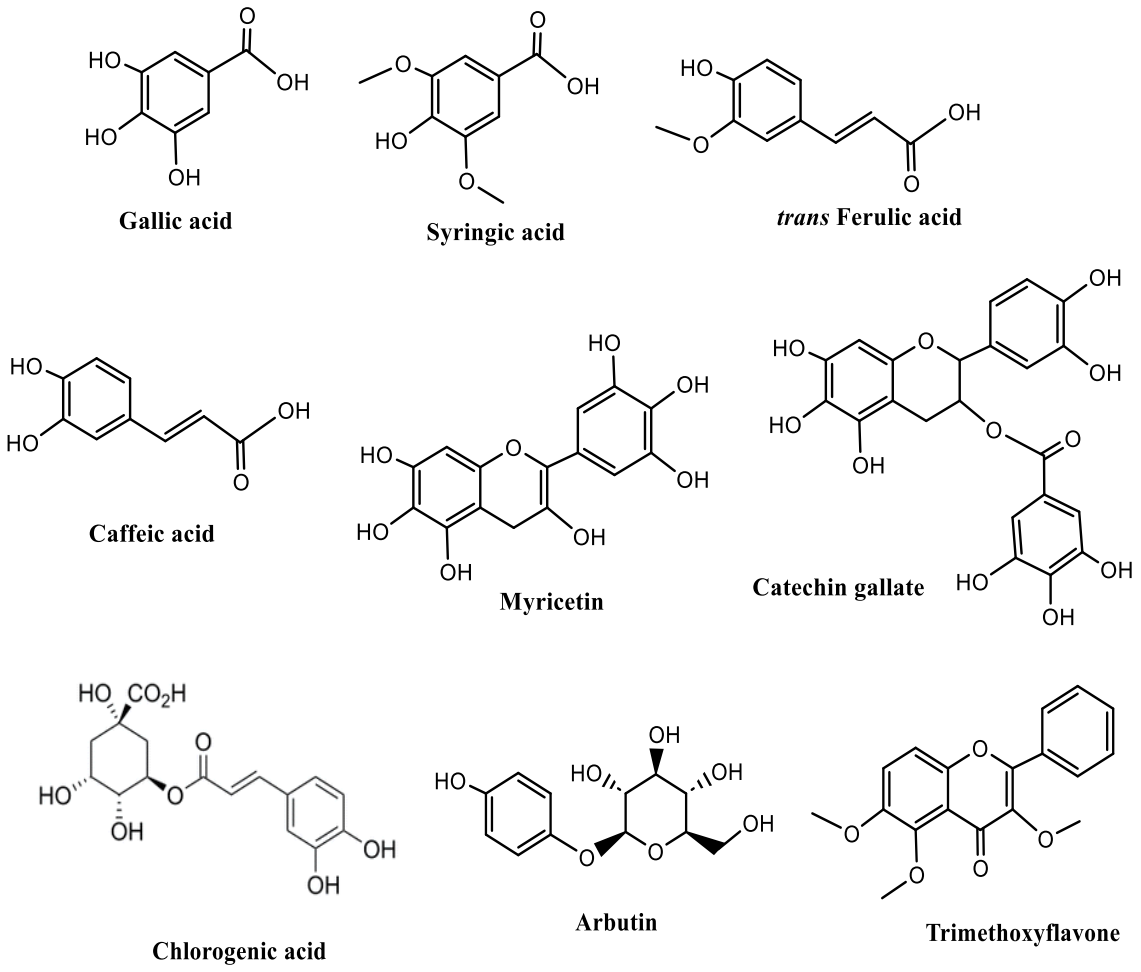

Figure I.11. Chemical structures of the identified compounds in *A. halimus* ethanolic extract

I.3.2.4. Traditional uses and Medicinal properties

In traditional medicine, *Atriplex halimus* is used to treat a wide range of diseases such as inflammation, cracked hands, hormones regulation, heart diseases, diabetes, and rheumatism [54, 55]. *A. halimus* extracts possess antimicrobial properties, effectively targeting a range of bacterial and fungal pathogens, making it a potential natural source for antimicrobial agents. Additionally, *Atriplex halimus* extracts are widely used to promote the healing of wounds and skin infections [56]. However, research remains limited on the cytotoxic activities of *A. halimus* extracts targeting breast cancer cell lines and their antioxidant properties [53].

I.3.2.5. Toxicity of the plant

Studies on mammalian cells have shown that *Atriplex halimus* extracts do not exhibit significant cytotoxic effects at concentrations up to 1 mg/mL [57, 58]. One potential concern with halophytes like *Atriplex halimus* is their capacity to accumulate heavy metals from the environment. Research indicates that *A. halimus* is indeed tolerant to heavy metals and is often explored for phytoremediation purposes, as it can absorb and accumulate metals such as cadmium, particularly in its roots. However, when cultivated under controlled or non-contaminated conditions, the heavy metal content in *Atriplex halimus* remains negligible, minimizing potential health risks associated with its use [59].

I.3.3. *Equisetum arvense* species

I.3.3.1. Description of the plant

The genus *Equisetum* is a genus of perennial plants that reproduce via spores rather than seeds, found throughout except in Australasia and Antarctica [60, 61]. There are about 30 known species, with the majority consisting of small plants, which rarely reach a meter in height. Its varied species are adapted to grow in temperate, tropical, and cold regions [62]. The species of the *Equisetum* genus are commonly referred to as "horsetail". The term is from Latin, combining “equi” (horse) and “setum” (tail), that is, horse tail [63]. *Equisetum arvense* (**Figure I.12**), commonly known as field horsetail or common horsetail, is a perennial herbaceous plant native to the temperate and Arctic regions of the Northern Hemisphere, especially Europe. It belongs to the Equisetopsida family and is easily recognized by its hollow, jointed stems and brush-like appearance [64].

Figure I.12. *Equisetum arvense* plant [65]

I.3.3.2. Botanical classification of *Equisetum arvense*

Equisetum arvense is classified botanically as follows:

- Kingdom: Plantae
- Division: Pteridophyta
- Class: Equisetopsida
- Order: Equisetales
- Family: Equisetaceae
- Genus: Equisetum
- Species: Equisetum arvense
- Arabic names: ذيل الحصان

I.3.3.3. Phytochemical composition of the plant

Equisetum arvense L. consists a variety of chemical components including silicic acid, linoleic acid, oleic acid, stearic acid, and minor quantities of alkaloids (e.g., equisetin, nicotine, palustrine, and palustrinine) (**Figure I.13**), glucosides, flavonoids, saponosides, triterpenoids, phytosterols, calcium carbonate, potassium sulfate, potassium chloride, manganese chloride, iron, manganese, and calcium phosphate [66].

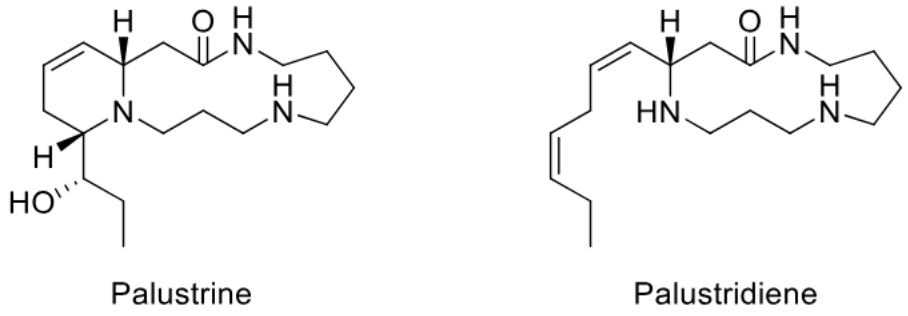

Figure I.13. Structures of known *Equisetum* alkaloids [67]

Mimica Duki investigated the phenolic composition of three extracts (EtOAc, *n*-BuOH, and aqueous). In this study, quercetin 3-*O*-glucoside (isoquercitrin) was the main components in EtOAc detected using high-performance liquid chromatography with diode-array detection (HPLC DAD). At the same time, apigenin 5-*O*-glucoside and kaempferol 3-*O*-glycoside were detected in considerable amounts. The *n*-BuOH extract showed higher amounts of isoquercitrin and di-*E*-caffeoyl-meso-tartaric acid, while the aqueous extract had di-*E*-caffeoyl-meso-tartaric acid and also two phenolic acids detected (**Figure I.14**) [68].

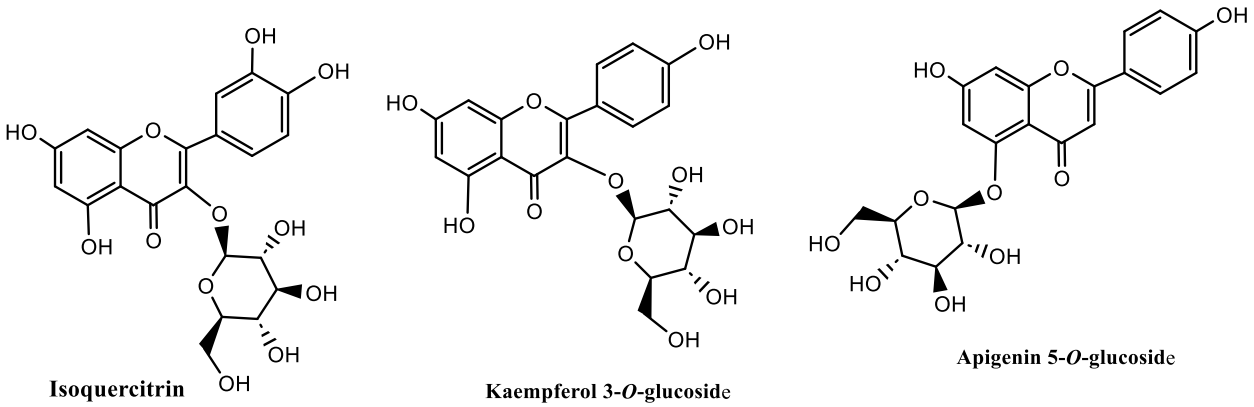

Figure I.14. Major Flavonoids in *Equisetum arvense*

I.3.3.4. Traditional uses and Medicinal properties

The most common traditional use of Equisetum is as a diuretic, followed by the treatment of genitourinary diseases (kidney diseases, urethritis, kidney stones, and others), inflammation, wound healing, rheumatic diseases, prostatitis, and hypertension [68]. *Equisetum arvense* possesses anticancer, antioxidant and anti-inflammatory properties, making it effective for treating inflammatory diseases like arthritis. Its flavonoid content offers to reduce oxidative stress and relieve pain. The plant rich in silica, which is essential for strong bones, joints, and connective tissues [69].

I.3.3.5. Toxicity of the plant

Tago et *al.* evaluated the toxicity of *E. arvense* in the diet at doses of 0, 0.3, 1, and 3% for 13 weeks in male and female rats. The dosage selections were based on estimated in take for humans, approximately 5mg/kg daily. No toxicity was detected related to clinical signs, body weight, urinalysis, hematology, serum biochemistry data, organ weights, and histopathological findings. Still, remedies containing *E. arvense* are not recommended during pregnancy or breastfeeding since little information is available on their safety. Indeed, the species contains thiaminase, an enzyme that destroys thiamine (vitamin B_1), and, with long-term use, could lead to vitamin deficiency, a possible cause of neurotoxicity [68].

References

[1] Mansoori, G.; Fauzi Soelaiman, T. Nanotechnology—An Introduction for the Standards Community. J. ASTM Int. 2005, 2, 1–22. https://doi.org/10.1520/JAI13110

[2] Gnash, A.; Lipinski, T.; Bednarkiewicz, A.; Rybka, J.; Capobianco, J.A. Upconverting nanoparticles: Assessing the toxicity. Chem. Soc. Rev. 2015, 44, 1561–1584. https://doi.org/10.1039/C4CS00177J

[3] National Nanotechnology Initiative (NNI). Available online: www.nano.gov (accessed on 22 July 2019).

[4] S. Bayda, M. Adeel, T. Tuccinardi, M. Cordani, F. Rizzolio, The History of Nanoscience and Nanotechnology: From Chemical–Physical Applications to Nanomedicine. Molecules, 2019, 27; 25(1). http://doi.10.3390/molecules25010112

[5] Allhoff, F. On the Autonomy and Justification of Nanoethics. *Nanoethics 2007, 1, 185–210.* Cite this article

[6] The British Museum. Available online: www.britishmuseum.org/research/collection_online/collection_object_details.aspx?objobjec=61219&partId=1 (accessed on 22 July 2019).

[7] Faraday, M. The Bakerian Lecture: Experimental Relations of Gold (and Other Metals) to Light. *Philos. Trans. R. Soc. Lond.* **1857***, 147, 145–181*. https://doi.org/10.1098/rstl.1857.0011

[8] Barhoum, A.; García-Betancourt, M.L.; Jeevanandam, J.; Hussien, E.A.; Mekkawy, S.A.; Mostafa, M.; Omran, M.M.; S. Abdalla, M.; Bechelany, M. Review on Natural, Incidental, Bioinspired, and Engineered Nanomaterials: History, Definitions, Classifications, Synthesis, Properties, Market, Toxicities, Risks, and Regulations. Nanomaterials 2022, 12(2), 177. https://doi.org/10.3390/nano12020177

[9] Mekuye B.; Abera B. Nanomaterials: An overview of synthesis, classification, characterization, and applications 2023. https://doi.org/10.1002/nano.202300038

[10] Nadeem Baig, Irshad Kammakakam and Wail Falath. Nanomaterials: a review of synthesis methods, properties, recent progress and challenges. Adv 2021, 2, 1821, 71. https://doi.org/10.1039/D0MA00807A

[11] A. A. Yaqoob, R. M. Khan, A. Saddique Int. J. Res 2019, 6, 7

[12] Khalid, K.; Tan, X.; Mohd, Z. H.F.; Tao, Y.; Lye, C. C.; Chu, D. T.; Lam, M. K.; Ho, Y. C.; Lim, J. W.; Wei, L. C. Advanced in developmental organic and inorganic nanomaterial, Bioengineered. 2020, 11, 328. https://doi.org/10.1080/21655979.2020.1736240

[13] Huynh, K. H.; Pham, X. H.; Kim, J.; Lee, S. H.; Chang, H.; Rho, W. Y.; Jun, B. H.; Int. J. Mol. Sci. 2020, 21, 5174. https://doi.org/10.3390/ijms21145174

[14] Dolez, I. editor. Nanoengineering: Global Approaches to Health and Safety Issues. Elsevier, Amsterdam, Netherland; 2015.

[15] Horikoshi, S.; Serpone, N. editors. Microwaves in Nanoparticle Synthesis: Fundamentals and Applications. John Wiley & Sons, Germany; 2013. https://doi.org/10.1002/9783527648122.ch1

[16] Ijaz, I.; Gilani, E.; Nazir, A.; Bukhari, A. Detail review on chemical, physical and green synthesis, classification, characterizations and applications of nanoparticles**.** Green Chem. Lett. Rev. 2020, 13, 223, 45. https://doi.org/10.1080/17518253.2020.1802517

[17] Cho, G.; Park, Y.; Hong, Y. K.; Ha, D. H. Ion exchange: an advanced synthetic method for complex nanoparticles, Nano. Converg. 2019. https://doi.org/10.1186/s40580-019-0187-0

[18] Findik, F. Nanomaterials and their applications. Period. Eng. Nat. Sci. 2021, 62, 75. https://doi.org/10.21533/PEN.V9I3.1837

[19] H. S Y. Khan, S. Z. Ali Shah, M. N. Khan, A. A. Shah, Classification, Synthetic, and Characterization Approaches to Nanoparticles, and Their Applications in Various Fields of Nanotechnology: A Review. Catalysts 2022, 12, 1386. https://doi.org/10.3390/catal12111386

[20] Baig, N.; Kammakakam, I.; Falath, Y. Nanomaterials: a review of synthesis methods, properties, recent progress, and challenges. Mater. Adv 2021, 2, 1821, 71. https://doi.org/10.1039/D0MA00807A

[21] Read SAK, Jimenez AS, Ross BL, Aitken RJ, von Tongeren M. Nanotechnology and exposure scenarios. In: Vogel U, Savolainen K, Wu Q, van Tongeren M, Brouwer D, Berges M, editors. Handbook of nanosafety-measurement, exposure and toxicology. Elsevier; 2013 https://doi.org/10.1016/B978-0-12-416604-2.00002-0

[22] Kaluza S, Kleine Balderhaar J, Orthen B, Honnert B, Jankowska E, Pietrowski P, et al. Workplace exposure to nanoparticles. In: Kosk-Bienko J, editor. European Agency for Safety and Health at Work; 2009. https://doi.org/10.13140/RG.2.1.3650.4487

[23] Hedmer M, Kåredal M, Gustavsson P, Rissler J. Carbon nanotubes. Arbete och Hälsa. Occupational and Environmental Medicine at Sahlgrenska Academy, University of Gothenburg; 2013. 252 p CNT_NEG_148_Carbon_nanotubes_2013

[24] Gugulothu, D.; Barhoum, A.; Afzal, S.M.; Venkateshwarlu, B.; Uludag, H. Structural Multifunctional Nanofibers and their Emerging Applications. In Handbook of Nanofibers; Springer: Berlin/Heidelberg, Germany, 2018; pp. 1–41.

[25] Sharma, V.K.; Filip, J.; Zboril, R.; Varma, R.S. Natural inorganic nanoparticles—Formation, fate, and toxicity in the environment. Chem. Soc. Rev. 2015, 44, 8410–8423. https://doi.org/10.1039/c5cs00236b

[26] Jeevanandam, J.; Barhoum, A.; Chan, Y.S.; Dufresne, A.; Danquah, M.K. Review on nanoparticles and nanostructured materials: History, sources, toxicity and regulations. Beilstein J. Nanotechnol. 2018, 9, 1050–1074. https://doi.org/10.3762/bjnano.9.98

[27] Lippmann, M. Effects of fiber characteristics on lung deposition, retention, and disease. In Proceedings of the Environmental Health Perspectives; US Department of Health and Human Services: Washington, DC, USA, 1990; Volume 88, pp. 311–317.

https://doi.org/ 10.1289/ehp.9088311

[28] Gurr, J.R.; Wang, A.S.S.; Chen, C.H.; Jan, K.Y. Ultrafine titanium dioxide particles in the absence of photoactivation can induce oxidative damage to human bronchial epithelial cells. Toxicology 2005, 213, 66–73. https://doi.org/10.1016/j.tox.2005.05.007

[29] Prasad, S.; Kumar, V.; Kirubanandam, S.; Barhoum, A. Engineered nanomaterials: Nanofabrication and surface functionalization. In Emerging Applications of Nanoparticles and Architectural Nanostructures: Current Prospects and Future Trends; Elsevier Inc.: Amsterdam, The Netherlands, 2018; pp. 305–340.

https://doi.org/10.1016/B978-0-323-51254-1.00011-7

[30] Lespes, G.; Faucher, S.; Slaveykova, V.I. Natural Nanoparticles, Anthropogenic Nanoparticles, Where Is the Frontier? Front. Environ. Sci. 2020, 8, 71. https://doi.org/10.3389/fenvs.2020.00071

[31] Grauso L, de Falco B, Lanzotti V, Motti R. Stinging nettle, Urtica dioica L.: botanical phytochemical and pharmacological overview. Phytochem Rev. 2020; 19:1341–77.

[32] Engelhardt L, Pöhnl T, Neugart S. Edible wild vegetables Urtica dioica L. and Aegopodium podagraria L.–antioxidants afected by processing. Plants. 2022; 11:2710. https://doi.org/10.3390/plants11202710.

[33] Parente, R., Paiva-Santos, A. C., Cabral, C and Costa, G. Comprehensive review of Urtica dioica L. (Urticaceae) phytochemistry and anti-inflammatory properties. Phytochemistry Reviews. 2024; 24:1591–1628. https://doi.org/10.1007/s11101-024-09980-6

[34] Randall, C., Meethan, K., Randall, H., & Dobbs, F. Nettle sting of Urtica dioica for joint pain – an exploratory study of this complementary therapy. Complementary Therapies in Medicine, (2000). 8(4), 237-241.

[35] Sharma, M., & Kaushal, J. Stinging nettle (Urtica dioica): Chemical composition, distribution, and applications in pharmaceutical and biomedical studies. Journal of Ethnopharmacology, (2016).179, 293-301

[36] Adhikari, B.M.; Bajracharya, A.; Shrestha, A.K. Comparison of nutritional properties of Stinging nettle (Urtica dioica) flour with wheat and barley flours. Food Sci. Nutr. 2016, 4, 119–124.

[37] Lapinskaya, E.S.; Kopytko, Y. Composition of the lipophilic fraction of stinging nettle (Urtica dioica L. and U. urens L.) homeopathic matrix tinctures. Pharm. Chem. J. 2008, 42, 699–702.

[38] Del Rio, D.; Rodriguez-Mateos, A.; Spencer, J.P.; Tognolini, M.; Borges, G.; Crozier, A. Dietary (poly)phenolics in human health: Structures, bioavailability, and evidence of protective effects against chronic diseases. Antioxid. Redox Signal. 2013, 18, 1818–1892.

[39] Pacifico, S.; Piccolella, S. Plant-Derived Polyphenols: A Chemopreventive and Chemoprotectant Worth-Exploring Resource in Toxicology. In Advances in Molecular Toxicology; Fishbein, J.C., Heilman, J.M., Eds.; Elsevier: Amsterdam, The Netherlands, 2015; pp. 161–214.

[40] Esposito, S.; Bianco, A.; Russo, R.; Di Maro, A.; Isernia, C and Pedone, P.V., Therapeutic Perspectives of Molecules from Urtica dioica Extracts for Cancer Treatment. Molecules 2019, 24, 2753.

[41] Đurovi´c, S.; Mici´c, D.; Šorgi´c, S.; Popov, S.; Gaši´c, U.; Tosti, T.; Kosti´c, M.; Smyatskaya, Y.A.; Blagojevi´c, S.; Zekovi´c, Z. Recovery of Polyphenolic Compounds and Vitamins from the Stinging Nettle Leaves: Thermal and Behavior and Biological Activity of Obtained Extracts. Molecules 2023, 28, 2278. https://doi.org/10.3390/molecules28052278

[42] Orˇci c, D.; Franciškovi´c, M.; Bekvalac, K.; Svirˇcev, E.; Beara, I.; Lesjak, M.; Mimica-Duki´c, N. Quantitative determination of plant phenolics in Urtica dioica extracts by high-performance liquid chromatography coupled with tandem mass spectrometric detection. Food Chem. 2014, 143, 48–53. https://doi.org/10.1016/j.foodchem.2013.07.097

[43] Veliˇckovi´c, V.; Đurovi´c, S.; Radojkovi´c, M.; Cvetanovi´c, A.; Švarc-Gaji´c, J.; Vuji´c, J.; Trifunovi´c, S.; Maškovi´c, P.Z. Application of conventional and non-conventional extraction approaches for extraction of Erica carnea L.: Chemical profile and biological activity of obtained extracts. J. Supercrit. Fluids 2017, 128, 331–337. https://doi.org/10.1016/j.supflu.2017.03.023

[44] Cvetanovi´c, A.; Švarc-Gaji´c, J.; Zekovi´c, Z.; Maškovi´c, P.; Đurovi´c, S.; Zengin, G.; Delerue-Matos, C.; Lozano-Sánchez, J.; Jakši´c, A. Chemical and biological insights on

aronia stems extracts obtained by different extraction techniques: From wastes to functional products. J. Supercrit. Fluids 2017, 128, 173–181. https://doi.org/10.1016/j.supflu.2017.05.023

[45] Đurovi'c´, S.; Koji´ c, I.; Radi´ c, D.; Smyatskaya, Y.A.; Bazarnova, J.G.; Filip, S.; Tosti, T. Chemical Constituents of Stinging Nettle (Urtica dioica L.): A Comprehensive Review on Phenolic and Polyphenolic Compounds and Their Bioactivity. Int. J. Mol. Sci. 2024, 25, 3430. https://doi.org/10.3390/ ijms25063430

[46] Semwal, P.; Abdur Rauf, Olatunde, A.; Singh, P.; Zaky, M.Y; Md. Islam, M.; Ahmed Khalil, A.; Abdullah S. M. Aljohani, Al Abdulmonem, W. and Ribaudo, G. The medicinal chemistry of Urtica dioica L.: from preliminary evidence to clinical studies supporting its neuroprotective activity: A review. Natural Products and Bioprospecting 2023, https://doi.org/10.1007/s13659-023-00380-5..

[47] Dar , S. A.; Ganai, F .A.; Yousuf, A. R.; Balkhi, A.U.H.; Bhat, T. M.; Sharma. S. Pharmacological and toxicological evaluation of Urtica dioica, 2013 ;51(2):170-80. https://doi.org/10.3109/13880209.2012.715172

[48] Balakrishnan, R. et al. "Anti-inflammatory and safety properties of nettle." Phytomedicine (2020).

[49] Siegers, C. P., et al. Allergic reactions to Urtica dioica. Toxicology Letters (2003).

[50] Bencheikh, N.; Elbouzidi, A.; Kharchoufa, L.; Ouassou, H.; Alami Merrouni, I.; Mechchate, H.; Es-Safi, I.; Hano, C.; Addi, M.; Bouhrim, M. Inventory of Medicinal Plants Used Traditionally to Manage Kidney Diseases in North-Eastern Morocco: Ethnobotanical Fieldwork and Pharmacological Evidence. Plants 2021, 10, 1966.

[51] Elbouzidi, A.; Bencheikh, N.; Seddoqi, S.; Bouhrim, M.; Bouramdane, Y.; Addi, M. Investigation of the Allelopathic Effect of Matricaria Chamomilla L. Parts' Aqueous Extracts on Germination and Seedling Growth of Two Moroccan Varieties of Durum Wheat. Int. J. Agron. 2021, 2021, 4451181.

[52] Bouchikh-Boucif, Y.; Labani, A.; Benabdeli, K.; Boidielouane, S. Allelopathic Effects of Shoot and Root Extracts from Three Alien and Native Chenopodiaceae Species on Lettuce Seed Germination. Ecol. Balk. 2014, 6, 51–55.

[53] Elbouzidi, A.; Ouassou, H.; Aherkou, M.; Kharchoufa, L.; Meskali, N.; Baraich, A.; Mechchate, H.; Bouhrim, M.; Idir, A.; Hano, C.; et al. LC–MS/MS Phytochemical Profiling, Antioxidant Activity, and Cytotoxicity of the Ethanolic Extract of Atriplex halimus L. against Breast Cancer Cell Lines: Computational Studies and Experimental Validation. Pharmaceuticals. 2022, 15, 1156.

[54] Mechaala, S.; Bouatrous, Y.; Adouane, S. Traditional Knowledge and Diversity of Wild Medicinal Plants in El Kantara's Area (Algerian Sahara Gate): An Ethnobotany Survey. Acta Ecol. Sin. 2021, 42, 33–45. https://doi.org/10.1016/j.chnaes.2021.01.007

[55] Walker, D.J.; Lutts, S.; Sánchez-García, M.; Correal, E. Atriplex halimus L.: Its Biology and Uses. J. Arid Environ. 2014, 100, 111–121. https://doi.org/10.1016/j.jaridenv.2013.09.004

[56] Rogers, M. E., Grieve, C. M., Shannon, M. C., & Francois, L. E. The effect of salinity and relative humidity on biomass production of *Atriplex halimus* and *Atriplex lentiformis*. *Environmental and Experimental Botany*, 2005, 54(3), 281-287.

[57] Amouroux, I., et al. "Safety evaluation of halophyte extracts. *Food and Chemical Toxicology* (2019).

[58] Ben Salem, H., et al. Medicinal and toxicological aspects of *Atriplex halimus*. *Pharmacognosy Reviews* (2011).

[59] Usman, K.; Al-Ghouti, M. A and Abu- Dieyeh. M. H. Phytoremediation: Halophytes as Promising Heavy Metal Hyperaccumulators, 2018.

[60] M. I. Calvo and R. Y. Cavero, "Medicinal plants used for cardiovascular diseases in Navarra and their validation from Official sources," Journal of Ethnopharmacology, vol. 157, pp. 268–273, 2014. https://doi.org/10.1016/j.jep.2014.09.047

[61] C. I. Wright, L. Van-Buren, C. I. Kroner, and M.M.G. Koning, «Herbal medicines as diuretics: a review of the scientific evidence," Journal of Ethnopharmacology, vol. 114, no. 1, pp. 1–31, 2007. https://doi.org/10.1016/j.jep.2007.07.023

[62] S. Olsen, Encyclopedia of Garden Ferns, Timber Press, Portland, OR, USA, 1st edition, 2007.

[63] W. B. Mors, C. Rizzini, and P. Pereira, Medicinal Plants of Brazil, Algonac: Reference Publications, Inc, Algonac, MI, USA, 2000.

[64] Cicero, A. F. G., & Derosa, G. Therapeutic applications of Equisetum in complementary and integrative health. Critical Reviews in *Food Science and Nutrition*, (2019). 59(10), 1507-1518.

[65] Pacific Northwest Flowers. Explore the flora of the Pacific Northwest. (2024), from https://www.pnwflowers.com/

[66] A. Asgharikhatooni, S. Bani, S. Hasanpoor et al., "e effect of equisetum arvense (horse tail) ointment on wound healing and pain intensity after episiotomy: a randomized placebo-controlled trial," Iranian Red Crescent Medical Journal, vol. 17, no. 3, pp. 1–7, 2015. https://doi.org/10.5812/ircmj.25637

[67] Cramer, L.; Ernst, L.; Lubienski, M.; Papke, U.; Schiebel, H.M.; Jerz, G.; Beuerle, T. Structural and Quantitative Analysis of Equisetum Alkaloids. Phytochemistry 2015, 116, 269–282. https://doi.org/10.1016/j.phytochem.2015.03.003

[68] Boeing, T.; Luisa Mota da Silva, Garcia, K.; Moreno, T.; Junior, A.G; and Souza, P. Phytochemistry and Pharmacology of the Genus Equisetum (Equisetaceae): A Narrative Review of the Species with Therapeutic Potential for Kidney Diseases, 2021, Article ID 6658434. https://doi.org/10.1155/2021/6658434

[69] Mohammed, H. I., Paray, B. A., & Rather, I. A. (2017). Anticancer activity of EA1 extracted from Equisetum arvense. In *Pak. J. Pharm. Sci*, 30 (5):1947-1950.

CHAPTER II

ZINC OXIDE NPs : SYNTHESIS, PROPERTIES AND CHARACTERIZATION METHODS

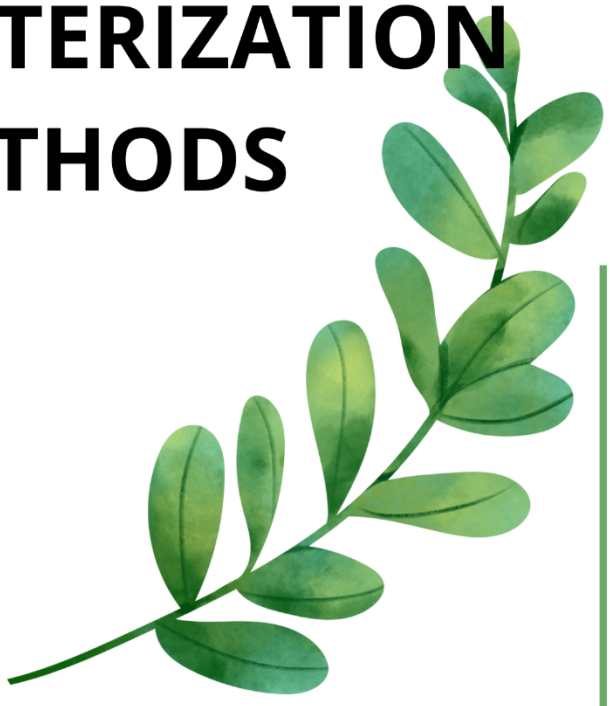

II.1. Overview of ZnO NPs

Zinc oxide, defined by the formula "ZnO," occurs naturally as zincite, a mineral frequently containing manganese and having a yellow to red tint. Its color varies according on its impurities; for example, its red color results from the presence of manganese, while in its pure form, it is transparent [1].

Figure II.1: Zinc Oxide (ZnO) in natural form.

Structurally, ZnO most commonly crystallizes in the hexagonal wurtzite form, which is stable at ambient conditions and imparts unique properties such as piezoelectricity and a wide direct band gap of approximately 3.37 eV at room temperature. These characteristics make ZnO a valuable semiconductor material with applications in optoelectronics, sensors, and transparent electrodes [2]. When synthesized at the nanoscale, zinc oxide nanoparticles (ZnO NPs) exhibit distinctive properties compared to their bulk counterpart, largely due to their high surface area-to-volume ratio and quantum size effects [3].

II.2. Properties of ZnO NPs and Their Importance

In recent years, ZnO NPs have generated significant research and industry attention due to their various characteristics that allow for applications in several industries. For example, ZnO NPs have been explored for gas sensing owing to their high chemical sensitivity, high electron mobility of 200 cm^2/V.s, and high thermal stability [4]. Their high exciton-binding energy of 60 meV has led to their use in photonic devices such as light-emitting devices (LEDs), photodiodes, and phototransistors [5]. The properties of ZnO NPs like transparency, low adhesiveness, and ability to

absorb ultraviolet (UV) light have allowed their use in cosmetics [6]. In the rubber industry, ZnO NPs are used as additives to enhance the properties of rubber such as strength, antiaging, and toughness, while their wide bandgap of 3.37 eV at (RT) results in their applications in optoelectronic devices such as supercapacitors [7, 8].

In addition, ZnO NPs exhibit antibacterial, anticancer, antioxidant, and anti-inflammatory properties, as well as being non-toxic and biocompatible [11]. Moreover, their capacity to absorb ultraviolet light and produce electron–hole pairs has resulted in their utilization as photocatalysts for the photodegradation of organic dyes and the generation of hydrogen gas via water-splitting [12, 13]. As shown in Table II.1, ZnO nanoparticles exhibit a hexagonal wurtzite crystal structure with distinctive lattice parameters that vary slightly depending on synthesis conditions. Their wide band gap and thermal stability make them particularly useful for optoelectronic applications [9,10].

Table II.1. Key physicochemical properties of zinc oxide nanoparticles (ZnO NPs)

Property	Value
Appearance	White solid
Odour	Odourless
Molecular weight	81.38 g/mol
Density	5.6 g/cm3
Coordination geometry	Tetrahedral
Crystal structure	Hexagonal wurtzite
Melting point	1975 ◦C (decomposes)
Flash point	1436 ◦C
Toxicity hazards	None
Refractive index	2.0041
Bandgap	3.37 eV
Electrical conductivity	Semiconductor
Hole effective mass	0.59
Electron effective mass	0.24
Exciton binding energy	60 meV
Bohr radius	2.34 nm
Luminescence	Luminescent in UV and visible light

II.3. Green Synthesis of ZnO NPs

Green chemistry has been defined by the United States Environmental Protection Agency (EPA) as "an area of chemistry, chemical engineering focused on the designing of chemical products or processes, which reduce the use of toxic substances" [14]. The green synthesis of NPs using plants, algae, and microorganisms is a green chemistry technology as it removes the necessity for hazardous raw materials and reduces the generation of toxic products [15]. It is an alternative method to the traditional synthesis methods that has attracted interest in recent years. Green synthesis of NPs using plants offers a more favorable option and has been explored for producing ZnO NPs with excellent results.

II.3.1. Biosynthesis of ZnO NPs using plant extracts

ZnO NPs have been synthesized using different plants and plant parts, with different zinc salts such as nitrates, chlorides, sulphates, and acetates as the Zn precursors (**Figure II.2**).

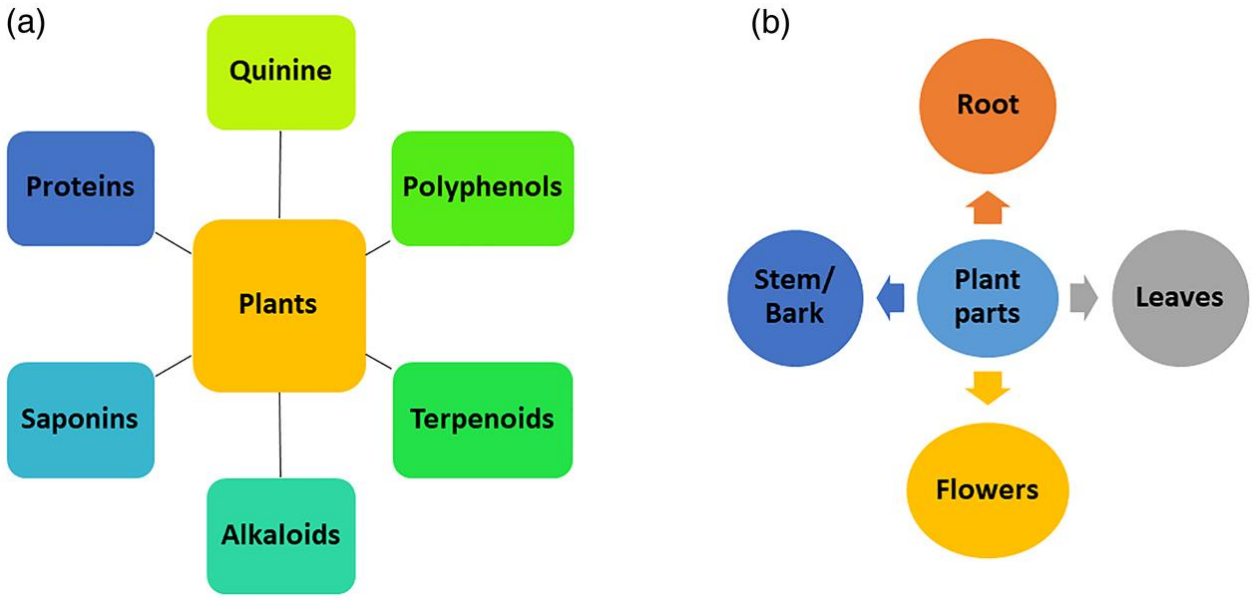

Figure II .2. Phytochemicals present in medicinal plants and different plant parts used in the synthesis of nanoparticles.

The synthesis process can be divided into three phases: **plant collection** and **treatment**, **biomolecule extraction**, and **synthesis**. The process of plant-mediated synthesis of ZnO nanoparticles is illustrated in Figure II.2.

The process begins with the collection of fresh plant material which is then washed to eliminate dirt and debris. The washed plant material is dried or used in its fresh form. The plant material is ground to powder to increase the interaction with the solvent during the extract process [16].

The biomolecule extraction step follows, utilizing green solvents like water and ethanol to isolate plant-derived compounds. The extraction is usually carried out at low temperatures (about 80 °C) using conventional extraction methods such as maceration, decoction, and Soxhlet extraction [16, 17].

After obtaining the plant extract, it mixed with the Zn salt precursor and heated at low temperatures. The reduction of the Zn salt precursors and the stabilization of the synthesized ZnO NPs by the plant biomolecules occurs in this step and the mechanism will be discussed in detail in later sections [16].

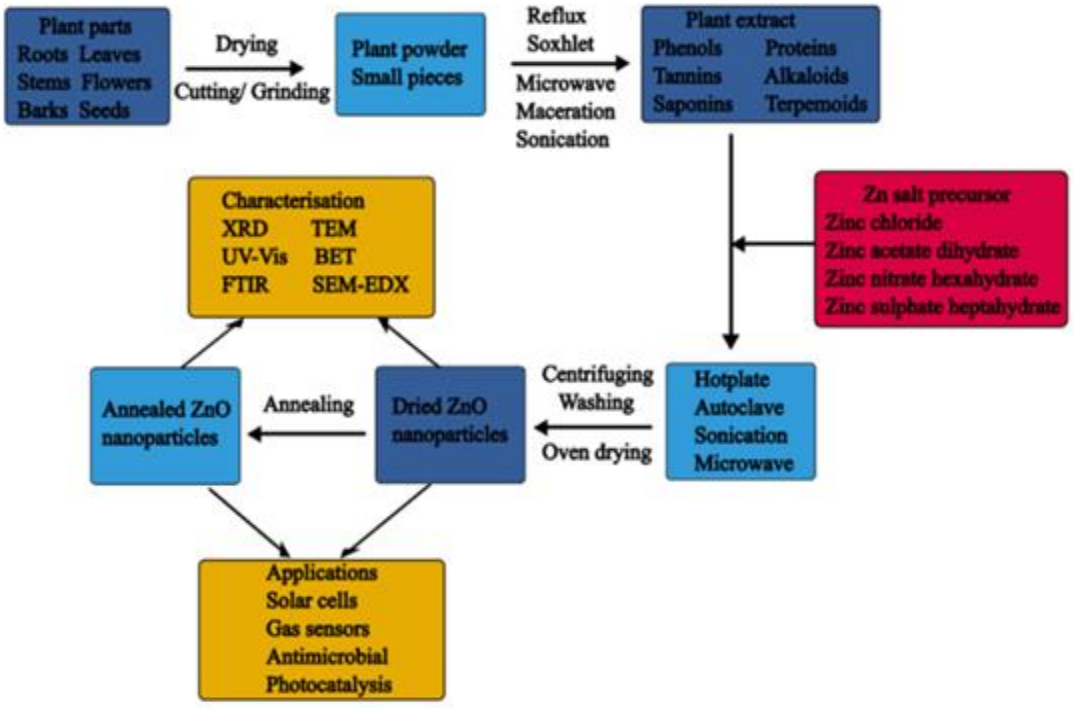

Figure II.3. Summary of plant-mediated synthesis of ZnO NPs

II.3.2. Pathways and Mechanisms of ZnO NPs Formation

Plant extracts contain bioactive compounds such as alkaloids, flavonoids, saponins, phenols, terpenoids, and tannins. These phytochemicals act as dual agents in green nanoparticle synthesis: their antioxidant properties facilitate the reduction of zinc salt precursors, while simultaneously stabilizing the resulting ZnO nanoparticles [18,19].

In general, the mechanism of synthesis of metal nanoparticles in plant extracts includes three main phases (**Figure II.4**) [20, 21].

- **The activation phase:** During this period the reduction of metal ions and the nucleation of reduced metal atoms occur.
- **The growth phase:** During this period, adjacent small nanoparticles spontaneously fuse into larger particles (directly by heterogeneous nucleation and growth and further reduction of metal ions; called Ostwald ripening), which is accompanied by an increase in the thermodynamic stability of the nanoparticles.
- **The termination phase:** The process determining the final shape of the nanoparticles

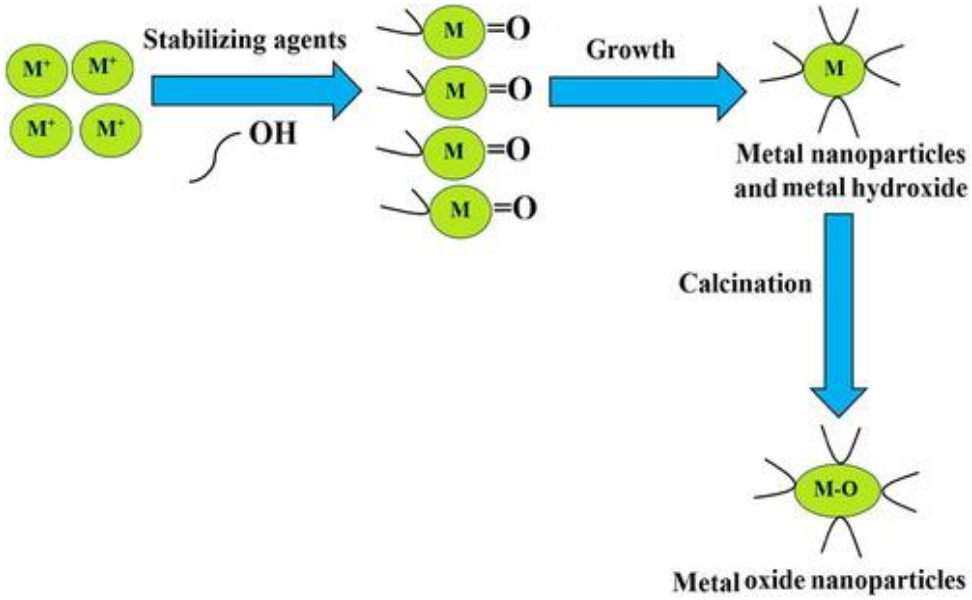

Figure II.4. Mechanism of green synthesis of metal oxide nanoparticles [22].

However, it should be noted that the mechanism of formation of ZnO NPs using plant extracts is not fully understood at the present moment. This is due to the presence of a large variety of biomolecules in the plant extracts, and the mechanism of formation is summarized in the following two equations:

$$(Zn^{2+}) + Biomolecule \rightarrow Zn - Biomolecule(complex) \quad (1)$$

$$Zn - Biomolecule(complex) \rightarrow ZnONPs \quad (2)$$

II.3.3. Synthesis Parameters Affecting Plant-Mediated ZnO NPs

The synthesis parameters such as pH, reaction time, precursor salt concentration, temperature, type of Zn salt precursor, and the influence of the type of biomolecules present in the extract and plant extract concentrations play a role in the formation of plant-mediated ZnO NPs and hence their properties [23].

- ✓ Type and concentration of salt precursor significantly affect the properties of nanoparticles during synthesis, with higher concentrations resulting in smaller particles and higher concentrations causing agglomeration [24].
- ✓ pH is an important parameter in nanoparticle synthesis, with multiple studies identifying pH 12 as optimal for the formation of ZnO NPs due to its influence on particle size, crystallinity, and stability. [25].
- ✓ Plant extract concentration has been reported to influence the properties of plant mediated ZnO NPs.
- ✓ Temperature is a crucial parameter in NP synthesis, as increasing reaction temperature decreases particle size due to favoring nucleation over growth at high temperatures.

II.3.4. The advantages and disadvantages of green synthesis of ZnO NPs

The green synthesis of zinc oxide nanoparticles (ZnO NPs) offers a sustainable alternative to traditional methods, balancing environmental benefits with some technical challenges. A detailed comparison in Table II.2 outlines its pros and cons:

Table II.2. The advantages and disadvantages of green synthesis of ZnO NPs [26].

Advantages	Disadvantages
Cost-effective	Reproducibility issues
Biocompatible	Relatively less stable NPs
Low energy consumption	Difficult to control morphology
Avoids hazardous chemicals	-
Does not require expensive equipment	-

II.4. Applications of ZnO NPs

Zinc oxide nanoparticles (ZnO NPs) possess a remarkable combination of physical, chemical, and biological properties that have led to their widespread application across diverse fields. The following organigram (Figure II.4) provides a clear overview of the main applications of ZnO nanoparticles:

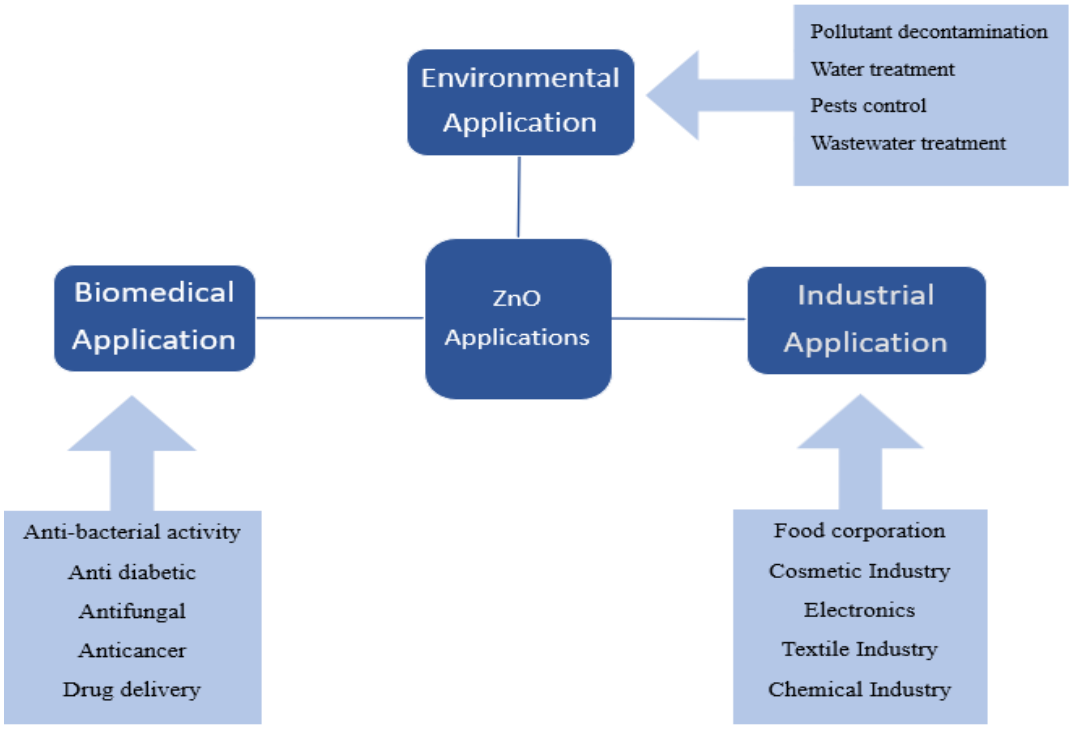

Figure II.5. Applications of ZnO-NPs [27]

II.4.1. Photocatalysis

II.4.1.1. Dyes and Wastewater Treatment Technologies

A dye is an organic molecule with a strong affinity for the substrate to which it is applied. Dyes impart color by absorbing specific wavelengths of visible light and reflecting or transmitting the remaining wavelengths, which are perceived as color by the human eye. The color-giving property of dyes is primarily due to the presence of chromophores-functional groups within the molecule that are responsible for absorbing light in the visible spectrum and thus imparting color [28,29].

Untreated industrial wastewater poses significant ecological, aquatic, and public health risks due to the persistence and toxicity of synthetic dyes. These dyes, which are resistant to biodegradation and breakdown by heat, light, or oxidation, accumulate in water systems, contaminating freshwater resources and disrupting ecosystems. With global freshwater supplies dwindling, there is an urgent need to develop effective wastewater treatment strategies. Conventional methods, such as aerobic and anaerobic processes, often fail to remove dye pollutants efficiently because of their stable chemical structures, rendering them inadequate for modern industrial demands This urgency has spurred research into innovative, cost-effective solutions capable of degrading or adsorbing these persistent pollutants to safeguard both environmental and human health [30].

II.4.1.2. Photocatalytic Mechanism of ZnO NPs

ZnO NPs have been utilized extensively for the photocatalytic degradation of dyes due to their properties such as having a low cost, high photostability, high chemical stability, high photoactivity in the UV region, high biological stability, and environmental friendliness [31]. These properties underpin their effectiveness in generating reactive oxygen species (ROS) under UV irradiation. When ZnO NPs are exposed to light energy equal to or exceeding their bandgap energy (~3.3 eV), electrons (e^-) in the valence band (VB) are excited to the conduction band (CB), leaving positively charged holes (h^+) in the VB (**Figure II.6**). The separated charge carriers migrate to the nanoparticle surface, where h^+ react with water or hydroxyl ions (OH^-) to produce hydroxyl radicals (·OH), while e^- reduce adsorbed oxygen to form superoxide radicals ($\cdot O_2^-$). These radicals further react to generate hydrogen peroxide (H_2O_2), which decomposes into additional ·OH. The resulting ROS, particularly

·OH, are highly oxidative and degrade adsorbed organic dyes into harmless byproducts like water and carbon dioxide (Equations 3–12). This mechanism makes it a robust solution for addressing persistent dye pollutants in wastewater [32, 33].

$$ZnO\ \ hv\ \rightarrow ZnO(h^+) + (e^-) \quad (3)$$

$$ZnO\ (h^+)\ + H_2O \rightarrow ZnO + (H^+) + (\cdot OH) \quad (4)$$

$$ZnO\ (h^+)\ + (OH^-)\ \rightarrow ZnO + (\cdot OH) \quad (5)$$

$$ZnO(e^-) + O_2\ \rightarrow ZnO + (\cdot {O_2}^-) \quad (6)$$

$$(\cdot {O_2}^-) + (H^+)\ \rightarrow \cdot HO_2 \quad (7)$$

$$\cdot HO_2\ + \cdot HO_2\ \rightarrow H_2O_2 + \ O_2 \quad (8)$$

$$ZnO(e^-) + H_2O_2 \rightarrow \cdot OH + (OH^-) \quad (9)$$

$$H_2O_2\ + (\cdot {O_2}^-) \rightarrow \cdot OH + (OH^-) + O_2 \quad (10)$$

$$H_2O_2 + hv\ \rightarrow 2 \cdot OH \quad (11)$$

$$\cdot OH + organic\ dyes\ \rightarrow\ mineral\ acids + CO_2\ + H_2O \quad (12)$$

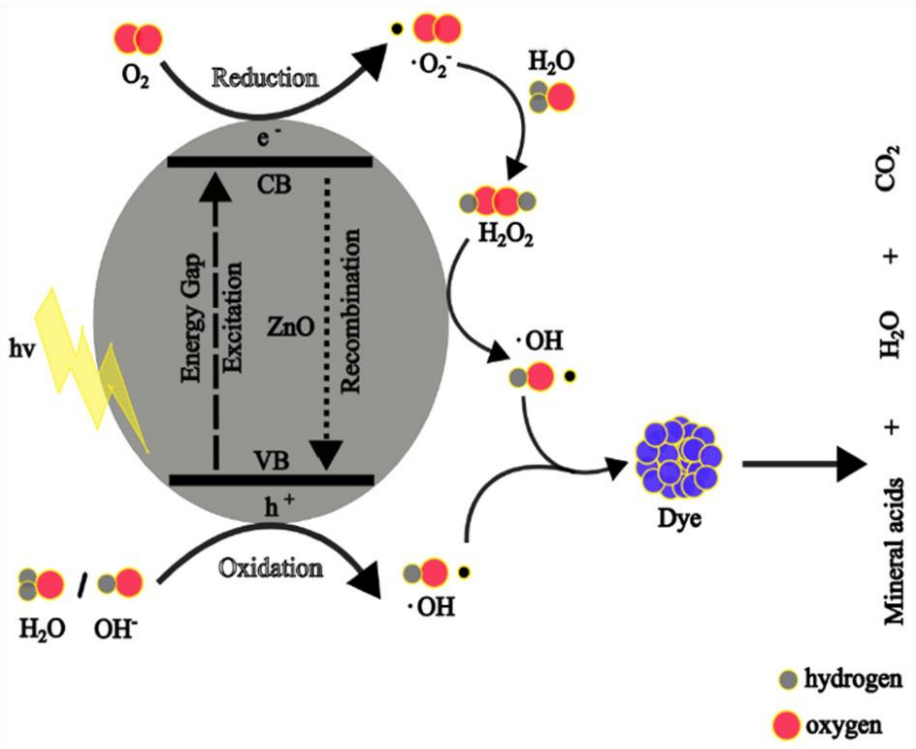

Figure II.6. Schematic diagram of the photocatalytic degradation mechanism of dyes using ZnO NPs.

The photocatalytic activity can be assessed using the percentage of degradation (efficiency), which indicates the degree of dye decomposition at any given time. It is achieved by measuring the maximum absorbance or concentration of the dye at a given time and can be represented using Equation (13).

$$\%\ \text{degradation efficiency} = \frac{Ao-At}{Ao} \times 100 = \frac{Co-Ct}{Co} \times 100 \qquad (13)$$

where $\mathbf{A_0}$ is the initial absorbance of the dye before photodegradation and $\mathbf{A_t}$ is the absorbance of the dye at time t, while $\mathbf{C_0}$ is the initial dye concentration and $\mathbf{C_t}$ is the dye concentration at time t.

II.4.1.3. Photocatalysis Activity of Plant-Mediated ZnO NPs

The particle size of nano-photocatalysts is one of the major factors that influence the photocatalytic activity of NPs. When the particle size of the nano-photocatalyst is small, there is a high surface area-to-volume ratio, which means increased active sites for the adsorption of surface oxygen and dye molecules, thus leading to better photoactivity [34].

The bandgap energy of nano-photocatalysts is crucial for their photocatalytic degradation activities. A small bandgap energy reduces energy needed to create charge carriers, allowing them to absorb more electromagnetic radiation, promoting hydroxyl radical generation and enhanced degradation. However, a balance is needed because a narrow bandgap energy leads to recombination of charge carriers, reducing hydroxyl radical generation and photodegradation [35]. Additionally, the shape of NPs has been reported to influence the photoactivity of the nano-photocatalysts.

II.5. Nanoparticles characterization

II.5.1. Analysis of Fourier-Transform Infrared Spectroscopy (FTIR)

Fourier Transform Infrared Spectroscopy (FTIR) is a non-destructive analysis technique based on the absorption of infrared radiation by the material to be analyzed [36]. It provides direct access to the molecular information and chemical nature of the material analyzed [37].

An FTIR spectrometer Shimadzu FTIR-8400S PC (**Figure II.7**) was used to study the chemical composition of the synthesized zinc nanoparticles. The dried powders of NPs were subjected to characterization in the range of 4000–400 cm^{-1} utilizing a KBr pellet strategy.

Figure II.7. Fourier-Transform Infrared Spectrometer

II.5.2. Analysis of UV-Vis

In this study, UV-visible absorption spectroscopy was performed using the PerkinElmer LAMBDA 950 UV/Vis/NIR spectrophotometer (**Figure II.8**). These measurements, performed at the Molecular and Environmental Chemistry Laboratory (LCME) of the University of Biskra, allow the determination of the optical band gap energy of the material. The absorption spectra were recorded in the spectral range from 200 to 800 nm, at room temperature.

Figure II.8. UV-Vis Spectrophotometer (PerkinElmer LAMBDA 950)

A band gap is the distance between the valence band of electrons and the conduction band. Essentially, the band gap represents the minimal energy that is required to excite an electron up to a state in the conduction band where it can participate in conduction [38]. The lower energy level is the valence band, and thus if a gap exists between this level and the higher energy conduction band, energy must be input for electrons to become free. The size and existence of this band gap allows one to visualize the distinction between conductors, semiconductors, and insulators [39], shown in (**Figure II.9).**

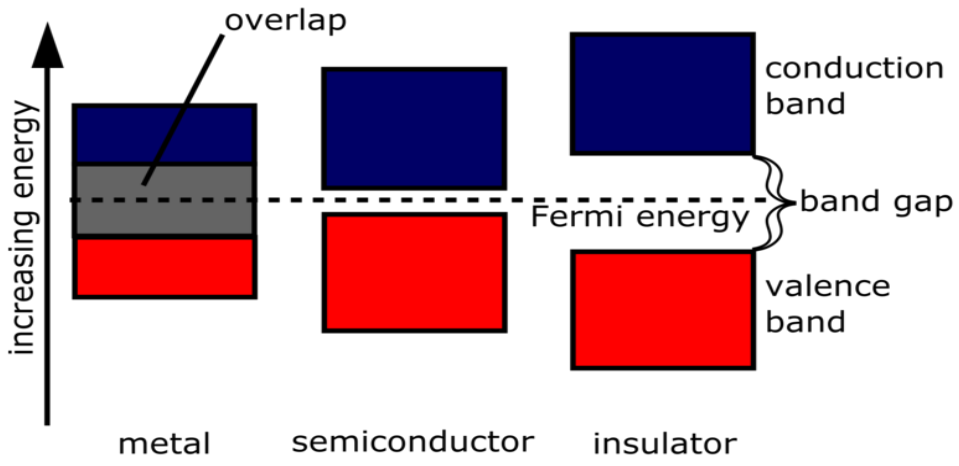

Figure II.9. A band gap diagram showing the different sizes of band gaps for conductors, semiconductors, and insulators [40].

The procedure of estimating the optical band gap is *via* the Tauc equation, which is a power-law expression in the form of Equation:

$$(\alpha h\nu)^{1\backslash n} = A(h\nu - Eg)$$

where **α** is absorption coefficient being a function of wavelength $\alpha(\lambda)$, $\boldsymbol{h}$ is Planck constant, $\boldsymbol{E_g}$ is an optical band gap of a semiconductor, $\boldsymbol{v}$ is frequency, $\boldsymbol{A}$ is proportionality constant, and $\boldsymbol{n}$ is Tauc exponent. Tauc coefficient is typically chosen as one of four values depending on the type of dominating transition in a studied semiconductor and according to the commonly used rules:

- $n = 1/2$; $n = 2$ for direct and indirect allowed transitions, respectively.
- $n = 3/2$; $n = 3$ for direct and indirect forbidden transitions, respectively.

The method involves plotting (αhv)1/n vs. hv and extrapolating the linear range beyond the absorption edge to determine the band gap on the abscissa axis. However, the value of n, and hence the nature of the transition, must be known [41].

II.5.3. Analysis of X-ray Diffraction (XRD)

The X-ray Diffraction (**Figure II.10**) analysis provides information on crystal structure, phase, crystallinity, texture, and average crystallite size. The XRD principle is based on the scattering of X-rays by crystal atoms, which results in the production of diffraction patterns and X-ray interferences. The interferences can be discovered using Bragg's law [42, 43].

$$n\lambda = 2d\,Sin\theta$$

This equation relates the wavelength (λ) of electro-magnetic radiation to the diffraction angle (θ) and the lattice spacing (d) in a crystalline sample [44].

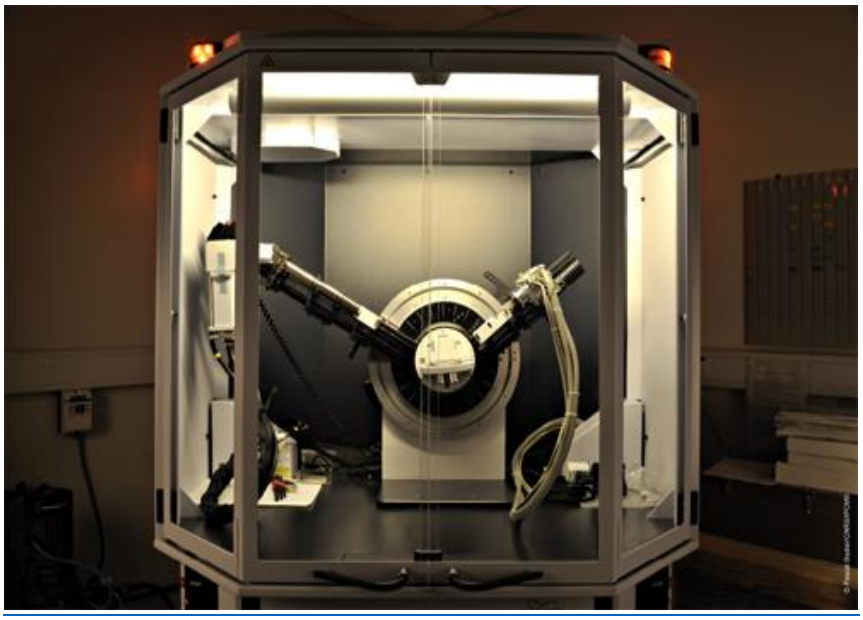

Figure II.10. XRD instrument

References

[1] http://physique.unice.fr/sem6/2013-2014/PagesWeb/PT/Heterostructure/page5.html

[2] Ü. Özgür, Y. I. Alivov, C. Liu, A. Teke, M. Reshchikov, S. Doğan, et al., A comprehensive review of ZnO materials and devices, Journal of applied physics, vol. 98, p. 11, 2005.

[3] K. S. Siddiqi, A.u. Rahman, Tajuddin and A. Husen, Properties of Zinc Oxide Nanoparticles and Their Activity Against Microbes, Nanoscale Research Letters. 2018, 13, 141. https://doi.org/10.1186/S11671-018-2532-3

[4] Al-darwesh, M.Y.; Ibrahim, S.S.; Faiad Naief, M.; Mishaal Mohammed, A.; Chebbi, H. Synthesis and Characterizations of Zinc Oxide Nanoparticles and Its Ability to Detect O_2 and NH_3 Gases. Results Chem. 2023, 6, 101064. https://doi.org/10.1016/j.rechem.2023.101064

[5] Nahhas, A.M. Introductory Chapter: Overview of ZnO Based Nano Materials and Devices. In Zinc Oxide Based Nano Materials and Devices; Nahhas, A., Ed.; Intechopen: Rijeka, Croatia, 2019. https://doi.org/10.5772/intechopen.85969

[6] Sonia, S.S.; Linda Jeeva Kumari, H.; Ruckmani, R.K.; Sivakumar, S.M. Antimicrobial and Antioxidant Potentials of Biosynthesized Colloidal Zinc Oxide Nanoparticles for a Fortified Cold Cream Formulation: A Potent Nanocosmeceutical Application. Mater. Sci. Eng. C 2017, 79, 581–589. https://doi.org/10.1016/j.msec.2017.05.059

[7] Dutta, G.; Sugumaran, A. Bioengineered Zinc Oxide Nanoparticles: Chemical, Green, Biological Fabrication Methods and Its Potential Biomedical Applications. J. Drug Deliv. Sci. Technol**.** 2021, 66, 102853. https://doi.org/10.1016/j.jddst.2021.102853

[8] Pradeeswari, K.; Venkatesan, A.; Pandi, P.; Karthik, K.; Hari Krishna, K.V.; Mohan Kumar, R. Study on the Electrochemical Performance of ZnO Nanoparticles Synthesized via Non-Aqueous Sol-Gel Route for Supercapacitor Applications. Mater. Res. Express **2019**, 6, 105525.

[9] Wojnarowicz, J.; Chudoba, T.; Lojkowski, W. A Review of Microwave Synthesis of Zinc Oxide Nanomaterials: Reactants, Process Parameters and Morphoslogies. Nanomaterials **2020**, 10, 1086. https://doi.org/10.3390/nano10061086

[10] Farahbod, F.; Farahmand, S. Empirical Investigation of Heating and Kinematic Performance of ZnO Nano Fluid in a Heat Pipe. J. Nanofluids 2017, 6, 128–135.

[11] Sharma, D.K.; Shukla, S.; Sharma, K.K.; Kumar, V. A Review on ZnO: Fundamental Properties and Applications. Mater. Today Proc. 2022, 49, 3028–3035. https://doi.org/10.1016/j.matpr.2020.10.238

[12] Bakranova, D.; Nagel, D. ZnO for Photoelectrochemical Hydrogen Generation. Clean. Technol. **2023**, 5, 1248–1268. https://doi.org/10.3390/cleantechnol5040063

[13] Dodoo-Arhin, D.; Asiedu, T.; Agyei-Tuffour, B.; Nyankson, E.; Obada, D.; Mwabora, J.M. Photocatalytic Degradation of Rhodamine Dyes Using Zinc Oxide Nanoparticles. *Mater. Today Proc. **2021**, 38, 809–815.* https://doi.org/10.1016/j.matpr.2020.04.597

[14] Nasrollahzadeh, M.; Sajjadi, M. An Introduction to Green Chemistry. In *Biopolymer-Based Metal Nanoparticle Chemistry for Sustainable Applications: Volume 1: Classification, Properties and Synthesis*; Elsevier: Amsterdam, The Netherlands, 2021; pp. 3–22. ISBN 9780128221082.

[15] Annu, A.A.; Ahmed, S. Green Synthesis of Metal, Metal Oxide Nanoparticles, and Their Various Applications. In *Handbook of Ecomaterials*; Springer International Publishing: Berlin/Heidelberg, Germany, 2019; Volume 4, pp. 2281–2325. ISBN 9783319682556

[16] https://iwaponline.com/view-large/figure/2687480/wst-em21767f01.tif

[17] Chennimalai, M.; Vijayalakshmi, V.; Senthil, T.S.; Sivakumar, N. One-Step Green Synthesis of ZnO Nanoparticles Using Opuntia Humifus Fruit Extract and Their Antibacterial Activities. *Mater. Today Proc. 2021, 47, 1842–1846.*

[18] Ahmed, S.; Annu; Chaudhry, S.A.; Ikram, S. A Review on Biogenic Synthesis of ZnO Nanoparticles Using Plant Extracts and Microbes: A Prospect towards Green Chemistry. *J. Photochem. Photobiol.* B 2017, 166, 272–284. https://doi.org/10.1016/j.jphotobiol.2016.12.011

[19] Bandeira, M.; Giovanela, M.; Roesch-Ely, M.; Devine, D.M.; da Silva Crespo, J. Green Synthesis of Zinc Oxide Nanoparticles: A Review of the Synthesis Methodology and Mechanism of Formation. *Sustain. Chem. Pharm*. 2020, 15, 100223.

[20] I. O. Minatel, C. V. Borges, M. I. Ferreira, H. A. G. Gomez, C.-Y. O. Chen, and G. P. P. Lima, "Phenolic compounds: Functional properties, impact of processing and bioavailability," Phenolic Compd. Biol. Act, pp. 1-24, 2017. https://doi.org/10.5772/66368

[21] S. Si and T. K. Mandal, "Tryptophan-based peptides to synthesize gold and silver nanoparticles: a mechanistic and kinetic study," Chemistry–A European Journal, vol. 13, pp. 3160-3168, 2007.

[22] Sabouri, Z.; Akbari, A.; Hosseini, H.A.; Khatami, M. and Darroudi, M. Green-based bio-synthesis of nickel oxide nanoparticles in Arabic gum and examination of their cytotoxicity, photocatalytic and antibacterial effects, Green Chemistry Letters and Reviews, (2021), 14:2, 404-414, DOI: 10.1080/17518253.2021.1923824. DOI: 10.1080/17518253.2021.1923824

[23] Fagier, M.A. Plant-Mediated Biosynthesis and Photocatalysis Activities of Zinc Oxide Nanoparticles: A Prospect towards Dyes Mineralization. *J. Nanotechnol*. 2021, 2021, 6629180.

[24] Al-Kordy, H.M.H.; Sabry, S.A.; Mabrouk, M.E.M. Statistical Optimization of Experimental Parameters for Extracellular Synthesis of Zinc Oxide Nanoparticles by a Novel Haloalaliphilic Alkalibacillus Sp. W7. *Sci. Rep*. 2021, 11, 10924. https://doi.org/10.1038/s41598-021-90408-y

[25] Abdullah, F.H.; Abu Bakar, N.H.H.; Abu Bakar, M. Low Temperature Biosynthesis of Crystalline Zinc Oxide Nanoparticles from Musa Acuminata Peel Extract for Visible-Light Degradation of Methylene Blue. *Optik* 2020, 206, 164279. https://doi.org/10.1016/j.ijleo.2020.164279

[26] Mutukwa, D.; Taziwa, R.T.; Khotseng, L. A Review of Plant-Mediated ZnO Nanoparticles for Photodegradation and Antibacterial Applications. Nanomaterials 2024, 14, 1182.

[27] Kundu, S.; Haydar, Md.S. and Mandal, P. Zinc Oxide Nanoparticles: Different synthesis approaches and applications. NBU Journal of Plant Sciences ISSN No. 0974-6927 Vol. 13(2021), pp. 42-64.

[28] Javaid, R.; Qazi, U.Y. Catalytic Oxidation Process for the Degradation of Synthetic Dyes: An Overview. Int. J. Environ. Res Public Health 2019, 16, 2066. https://doi.org/10.3390/ijerph16112066

[29] Kumar, A.; Dixit, U.; Singh, K.; Prakash Gupta, S.; Beg, M.S.J. Structure and Properties of Dyes and Pigments. In Dyes and Pigments; Papadakis, R., Ed.; Intechopen: London, UK, 2021.

[30] Al-Tohamy, R.; Sameh S. Ali, Fanghua Li, Kamal M. Okasha, Yehia A.-G. Mahmoud, Tamer Elsamahy, Haixin Jiao, Yinyi Fu, Jianzhong Sun. A critical review on the treatment of dye-containing wastewater: Ecotoxicological and health concerns of textile dyes and possible remediation approaches for environmental safety, Ecotoxicology and Environmental Safety Vol 231, 2022, 113160. https://doi.org/10.1016/j.ecoenv.2021.113160

[31] Lanjwani, M.F.; Tuzen, M.; Khuhawar, M.Y.; Saleh, T.A. Trends in Photocatalytic Degradation of Organic Dye Pollutants Using Nanoparticles: A Review. Inorg. Chem. Commun. 2024, 159, 111613. https://doi.org/10.1016/j.inoche.2023.111613

[32] Fagier, M.A. Plant-Mediated Biosynthesis and Photocatalysis Activities of Zinc Oxide Nanoparticles: A Prospect towards Dyes Mineralization. J. Nanotechnol. 2021, 2021, 6629180. https://doi.org/10.1155/2021/6629180

[33] Ong, C.B.; Ng, L.Y.; Mohammad, A.W. A Review of ZnO Nanoparticles as Solar Photocatalysts: Synthesis, Mechanisms and Applications. Renew. Sustain. Energy Rev. 2018, 81, 536–551. https://doi.org/10.1016/j.rser.2017.08.020

[34] Gangwar, J.; Sebastian, J.K. Unlocking the Potential of Biosynthesized Zinc Oxide Nanoparticles for Degradation of Synthetic Organic Dyes as Wastewater Pollutants. Water Sci. Technol. 2021, 84, 3286–3310. https://doi.org/10.2166/wst.2021.430

[35] Bhattacharjee, N.; Som, I.; Saha, R.; Mondal, S. A Critical Review on Novel Eco-Friendly Green Approach to Synthesize Zinc Oxide Nanoparticles for Photocatalytic Degradation of Water Pollutants. Int. J. Environ. Anal. Chem. 2022, 104, 489–516. https://doi.org/10.1080/03067319.2021.2022130

[36] F. Bouanaka, "Optical emission spectroscopy (OES) by multichannel optical analyzer of a low-pressure plasma," (2008).

[37] A. Zaradi, Elaboration de spinelle MgAl2O4 à partir de nanopoudres synthétisées, thèse doctorat, Université Ferhat Abbas - Sétif 1, Algérie, 2019. http://dspace.univ-setif.dz:8888/jspui/handle/123456789/3515

[38] PV Education. (September 26, 2015). *Band Gap* [Online]. Available: http://www.pveducation.org/pvcdrom/pn-junction/band-gap

[39] HyperPhysics. (September 26, 2015). *Band Theory of Solids* [Online]. Available: http://hyperphysics.phy-astr.gsu.edu/hbase/solids/band.html

[40] Wikimedia Commons. (September 26, 2015). *Band Gap Comparison* [Online]. Available: https://upload.wikimedia.org/wikipedia/commons/thumb/0/0b/Band_gap_comparison.svg/2000px-Band_gap_comparison.svg.png

[41] Haryński, Ł.; Olejnik, A.; Grochowska, K.; Siuzdak, K. "A facile method for Tauc exponent and corresponding electronic transitions determination in semiconductors directly from UV–Vis spectroscopy data", Optical Materials, 2022, 112205.

[42] Bunaciu, A.A.; Udri¸ stioiu, E.; Aboul-Enein, H.Y. X-ray Diffraction: Instrumentation and Applications. Crit. Rev. Anal. Chem. 2015, 45, 289–299. https://doi.org/10.1080/10408347.2014.949616

[43] Rajeshkumar, S.; Bharath, L.V. Mechanism of Plant-Mediated Synthesis of Silver Nanoparticles. A Review on Biomolecules Involved, Characterization and Antibacterial Activity. Chem. Biol. Interact 2017, 273, 219–227. https://doi.org/10.1016/j.cbi.2017.06.019

[44] Boddolla, S. and Thodeti, S. A review on Characterization techniques of Nanomaterials. *International Journal of Engineering, Science and Mathematics*, Vol. 7 Issue1, 2018, ISSN: 2320-0294: 6.76. http://www.ijesm.co.in

CHAPTER III

MATERIALS AND METHODS

III.1. Study Overview

This research focuses on the eco-friendly synthesis of zinc oxide nanoparticles (ZnO NPs) using aqueous extracts of three medicinal plants: *Urtica dioica* (stinging nettle), *Atriplex halimus* (saltbush), and *Equisetum arvense* (horsetail). The work is conducted at the Laboratory of Chemistry, Faculty of Exact Sciences and Materials Science, University of Biskra, Algeria. The study aims to develop sustainable ZnO NPs with optimized structural, optical, and functional properties for enhanced photocatalytic degradation of environmental pollutants. The research is structured as follows:

1. **Synthesis of ZnO Nanoparticles**
    - Optimization of green synthesis parameters (pH, temperature, extract concentration).
    - Utilization of plant-derived phytochemicals as reducing and stabilizing agents.

2. **Characterization of ZnO NPs**
    - **Optical properties**: UV-Visible spectroscopy (UV-Vis) for bandgap analysis.
    - **Functional groups**: Fourier-transform infrared spectroscopy (FTIR) to identify bioactive molecules involved in synthesis.
    - **Crystallinity and phase**: X-ray diffraction (XRD) for crystal structure and size determination.

3. **Photocatalytic Applications**
    - Evaluation of ZnO NP efficiency in degrading organic dyes (Rhodamine B) under sun light.
    - Correlation of nanoparticle properties (size, surface area, crystallinity) with photocatalytic performance.

III.2. Green synthesis of ZnO NPs

III.2.1. Materials and Product

Laboratory equipment

- Electric balance
- Magnetic stirrer
- Static oven
- Centrifuge
- Beakers
- Watch glass
- Spatula
- Funnel
- Glass stirring rod
- Erlenmeyer flask
- Magnetic stirrer
- Filter paper
- Measuring cylinders
- Aluminum foil
- Tubes

Chemical products

Zinc chloride (0.1M), Sodium hydroxide (2M), Dyes (Crystal Violet and Rhodamine B)

III.2.2. Preparation of plant extracts

Fresh aerial parts of *Urtica dioica*, *Atriplex halimus*, and *Equisetum arvense* were individually and thoroughly washed with distilled water to remove dust and impurities. The cleaned plant materials were then air-dried in a shaded, well-ventilated area to preserve their bioactive constituents. Once completely dried, the samples were finely ground into powder to maximize the surface area for extraction. For each plant, 30 grams of the powdered material were mixed with 300 mL of deionized water in a beaker and subjected to maceration at room temperature for 48 hours; this extraction process was repeated at least twice to ensure maximum yield. The resulting mixtures were first filtered to remove solid residues and then centrifuged at 4000 rpm for 30 minutes to obtain clear plant extracts for subsequent use (**Figures III.1**, **III.2**, and **III.3**).

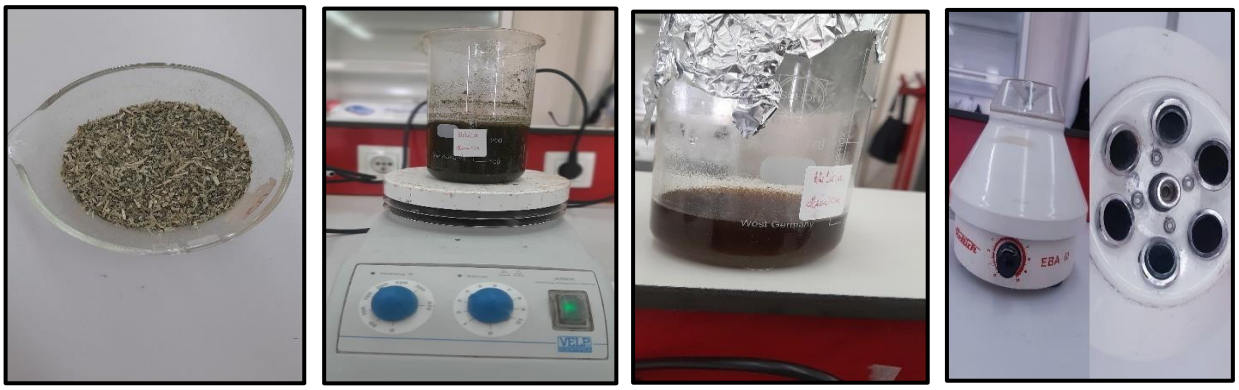

Figure III.1. Preparation Steps for *Urtica dioica* (Nettle) Extract

Figure III.2. Preparation Steps for *Atriplex halimus* (Saltbush) extract

Figures III.3. Preparation Steps for *Equisetum arvense* (Horsetail) extract

III.2.3. Green synthesis of ZnO using plant extracts

The green synthesis of ZnO nanoparticles using plant extracts comprises the following key steps (**Figure III.4**):

a. Preparation of Zinc Chloride Solution (0,1 M)

A quantity of 1.36 g of zinc chloride is dissolved in 100 mL of distilled water with continuous stirring at room temperature until a homogeneous solution is obtained.

b. Reaction Setup

A 100 mL volume of zinc chloride solution (0.1 M) was heated to 90°C under continuous stirring. To this, 100 mL of plant extract was added dropwise, and the mixture was maintained at 90°C for 4 hours. Subsequently, a sodium hydroxide solution (2 M) was gradually added until the pH reached 12, as monitored using a calibrated pH paper.

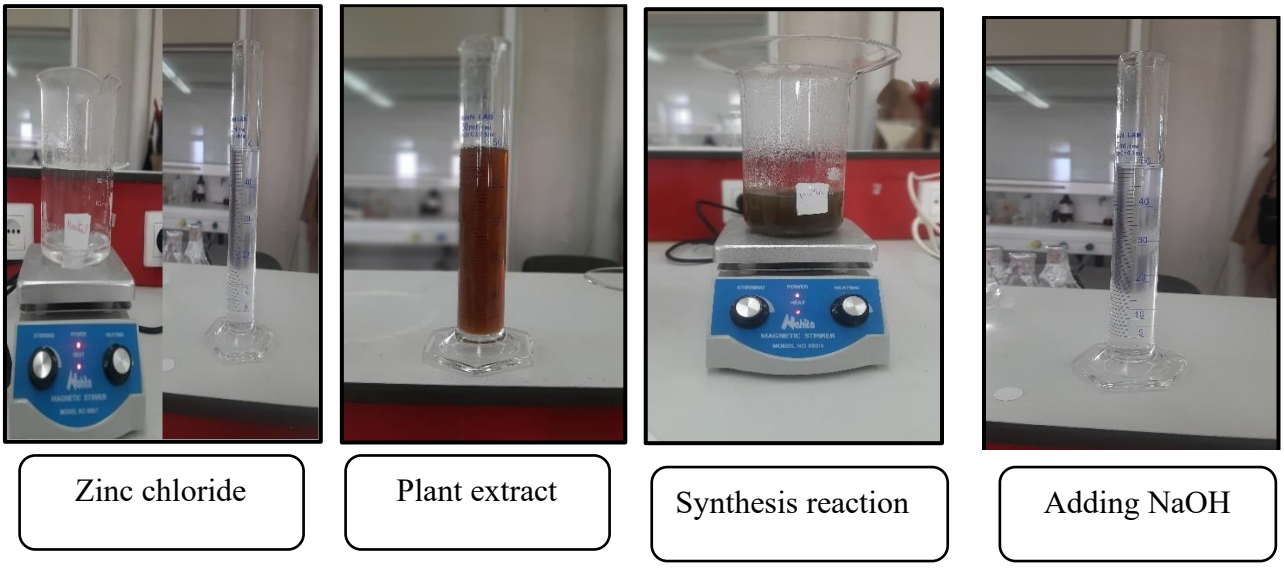

Figures III.4. Reaction Setup for the green synthesis of ZnO Nanoparticles

c. Precipitation and purification

The mixture was allowed to cool to room temperature, then centrifuged at 6000 rpm for 40 minutes. The resulting precipitate was washed twice with distilled water to remove any remaining impurities (**Figure III.5**).

Figures III.5. Precipitation step

d. Drying and processing

The purified ZnO nanoparticles were dried in an oven at 65 °C overnight, then ground into a fine powder using a mortar and pestle to obtain the final zinc oxide nanoparticles.

Figures III.6. Drying steps

All these steps are repeated for each plant extract, as well as for the mixture of the three plants.

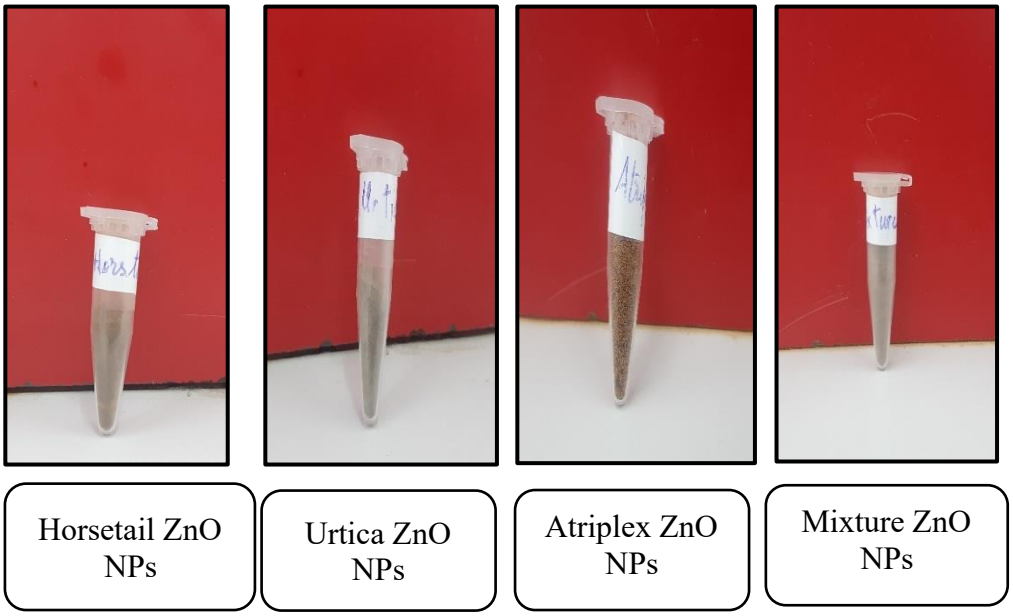

Figures III.7. Powders of Synthesized ZnO Nanoparticles

e. Calcination step

All those powders are calcined in a muffler at T= 450°.

III.2. Photocatalytic ZnO NPs application (Rhodamine B degradation study by synthesized ZnO NPs)

III.2.1. What is Rhodamine B

Rhodamine B (RhB) which is the most commonly used dye in food, paper, printing, pharmaceuticals, and textiles. It belongs to the xanthene dye family, which is unsafe for living organisms. It is noxious causing mutagenic and carcinogenic effect of living organisms [1].

Table. III.3: Properties and molecular structure of Rhodamine B

Properties	
Chemical formula	$C_{28}H_{31}Cl\ N_2O_3$
Molar mass	479,02 g/mol
Melting point	210 to 211 °C (410 to 412 °F; 483 to 484 K) (Decomposes)
Solubility in water	8 g/L and ~15 g/L
Absorption maximum	553.60 nm
Molecular structure	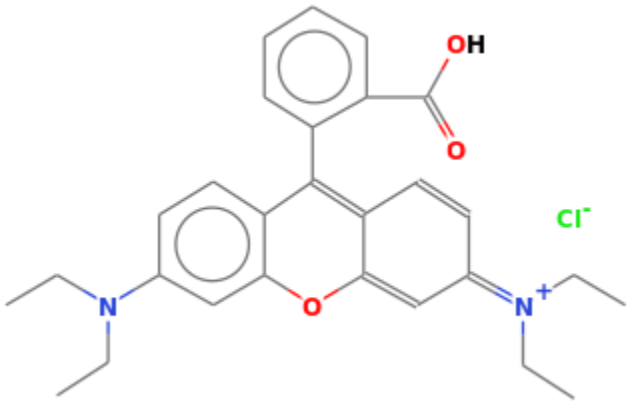

III.2.2. Photocatalytic evaluation

a- Experimental Conditions:

- **Pollutant:** Rhodamine B (RhB),
- **Photocatalyst**: ZnO nanoparticles biosynthesized from (Atriplex, Urtica, Horsetail and their mixture).
- **Irradiation Source**: Sunlight (April 2025).
- **Initial RhB Concentration**: 5mg/L.
- **Catalyst Dose**: 0,1g
- **Room Temperature**.
- **Magnetic Stirring**: Moderate.
- **Treatment Time**: 3h (180min).

b- Experimental approach

The photocatalytic activity of the synthesized ZnO nanoparticles was evaluated using the degradation of Rhodamine B dye under sunlight. 0.1g of ZnO NPs was dispersed in 100 mL of 5 mg/L Rhodamine B aqueous solution. Prior to irradiation, the suspension was magnetically stirred in the dark for 30 minutes to establish adsorption–desorption equilibrium. The reaction mixture was then exposed to sunlight under constant stirring. At regular time intervals (30 minutes), 4 mL aliquots were withdrawn in aluminum-coated tubes, then centrifuged to remove the catalyst, and the absorbance of the supernatant was measured using a UV-Vis spectrophotometer to monitor the degradation of Rhodamine B.

References

[1] Sudhaik, A.; Raizada, P.; Ahamad, T.; Alshehri, S. M.; Nguyen, V. H.; Van Le, Q.; Thakur, S.; Thakur, V. K. Recent advances in cellulose supported photocatalysis for pollutant mitigation: A review, Vol 226, 2023, P 1284-1308. https://doi.org/10.1016/j.ijbiomac.2022.11.241

CHAPTER IV

RESULTS AND DISCUSSION

IV.1. ZnO Nanoparticles characterization

IV.1.1. Analysis of Fourier-Transform Infrared Spectroscopy (FTIR)

The FTIR analysis was performed using an FTIR spectrophotometer (FTIR-8400S, Shimadzu) in the frequency range of 4000–400 cm^{-1}. The infrared (IR) spectrum **(Figure IV.1)** confirms the successful formation of zinc oxide (ZnO) nanoparticles biosynthesized using plant extracts from *Atriplex halimus*, *Urtica dioica*, *Equisetum arvense*, and their mixture. Key functional groups identified in the spectrum include [1–4]:

- A broad peak observed between **3500–3000 cm^{-1}** in the calcined ZnO bionanoparticles is attributed to the stretching vibrations of surface hydroxyl groups (–OH) chemically bound to the ZnO surface. This band may also arise from **residual organic compounds** (e.g., phenolics, alcohols, or carboxylic acids) present in the plant extracts that were not fully decomposed at 400 °C, and/or **hydrogen-bonded hydroxyl groups**.
- A band around **2420 cm^{-1}** is attributed to symmetric and asymmetric **C–H** stretching vibrations.
- A prominent band observed at **1600 cm^{-1}** is assigned to C=O (carbonyl) stretching in polyphenols, proteins, and other bioactive molecules from the plant extracts.
- A band located between **1350–1450 cm^{-1}** is associated with **C-H** bending vibrations or **carboxylate (COO^-)** groups, further highlighting the role of carboxylic acids or related organic functional groups in the biosynthesis process.
- Observable weak peaks **at 850–1100 cm^{-1}** confirm the presence of **C–O** stretching in amino acid and **C–H** bending, respectively.
- The distinct peak between **440–550 cm^{-1}** matches the vibrational mode of **ZnO**, confirming nanoparticle formation.

The spectroscopic characterization by IR has revealed all the chemical bonds present in the ZnO nanoparticles, and these bonds are similar across all samples prepared from different plant sources.

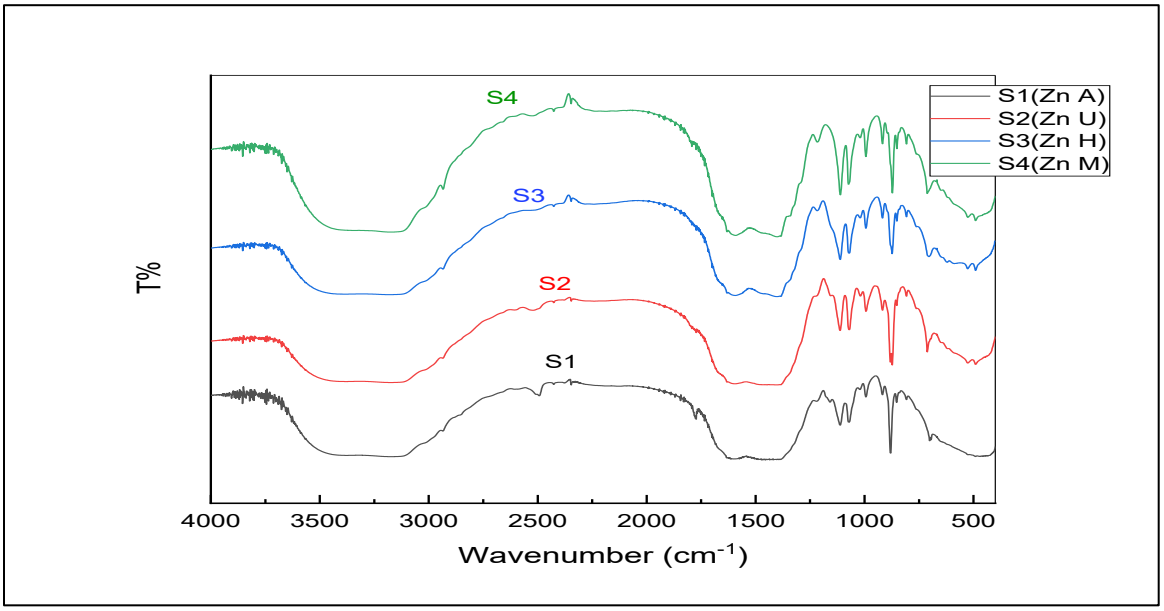

Figure IV.1. FTIR spectra of (S1) Atriplex ZnO NPs; (S2) Urtica ZnO NPs; (S3) Horsetail ZnO NPs and (S4) mixture ZnO NPs.

The results confirm that phenols, polyphenols, and primary amines from plant extracts play a critical role in capping and stabilizing the synthesized ZnO nanoparticles. The persistence of these compounds in the final product suggests **incomplete decomposition**, likely due to insufficient calcination time or temperature during synthesis. To investigate this hypothesis, zinc oxide extracted from *Urtica dioica* was washed with distilled water and ethanol (1:1 ratio), centrifuged, dried, and divided into two batches:

a) **S1**: Calcined at 600 °C.

b) **S2**: Calcined at 800 °C.

FTIR **(Figure IV.2)** analysis of both samples revealed:

- S1 (600 °C): Retained residual organic functional groups (e.g., C=O, C–H) from the plant extract, confirming incomplete decomposition.
- S2 (800 °C): Exhibited a stronger Zn–O vibrational band (**440–550 $\mathbf{cm^{-1}}$**) and minimal organic peaks, indicating near-complete removal of capping agents.

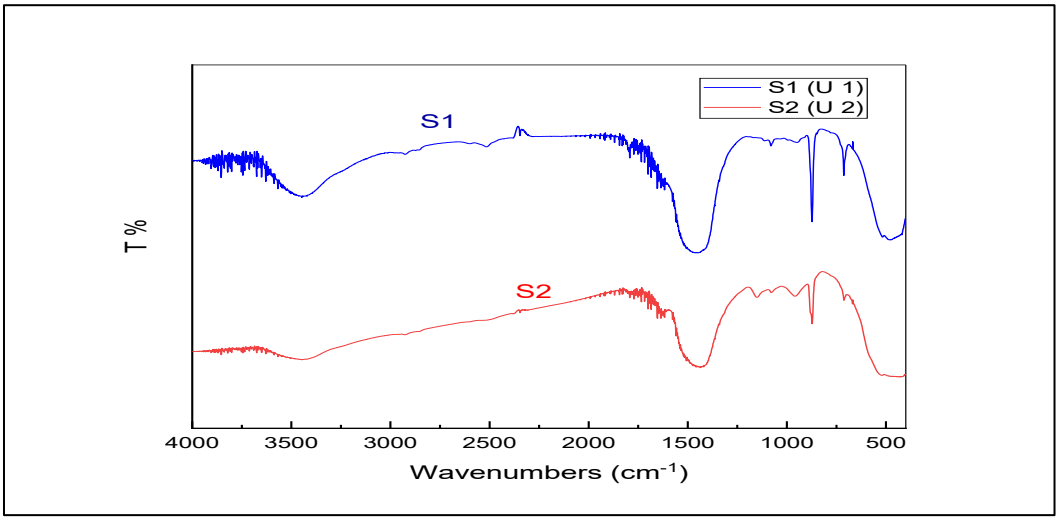

Figure.IV.2. FTIR spectra of calcined *Urtica dioica* ZnO nanoparticles (S1: 600 °C; S2: 800 °C)

The key bands can be summarized in the **table IV.1** as follows:

Table.IV.1: Key FTIR Bands and Attributions for Calcined *Urtica dioica* ZnO Nanoparticles

Band(cm^{-1})	**Attribution**	**S1 vs S2**	**Reference**
3200–3600	O–H stretching (water, hydroxyls, phenolic OH)	Broad in S1 (hydroxyl/water from organics); much weaker or gone in S2.	[5]
1600–1650	C=O stretching (carbonyls, amide I) or aromatic C=C	Clear in S1 (e.g. proteins/phenolics); greatly diminished in S2.	-
1500–1580	Aromatic C=C, N–H bending (amide II), or C–O stretching	Seen in S1; weak or absent in S2.	[5]
1380–1470	C–H bending, phenolic C–O	Broad band in S1; weak or gone in S2.	[5]
1100–1300	C–O / C–C stretching (ethers, esters, alcohols)	Overlap of organics in S1; virtually absent in S2.	[5, 6]
~470–570	Zn–O lattice vibration	Strong in both; S1 ≈476 cm^{-1}, S2 ≈477 cm^{-1} (slight blueshift and sharpening in S2).	[5, 6]

IV.1.2. Analysis of XRD

Figure IV.3 presents the XRD patterns of ZnO nanoparticles synthesized at 90 °C for 4 hours. The X-ray diffraction analysis confirms the crystalline nature of the ZnO nanoparticles, as evidenced by the well-defined and broadened diffraction peaks.

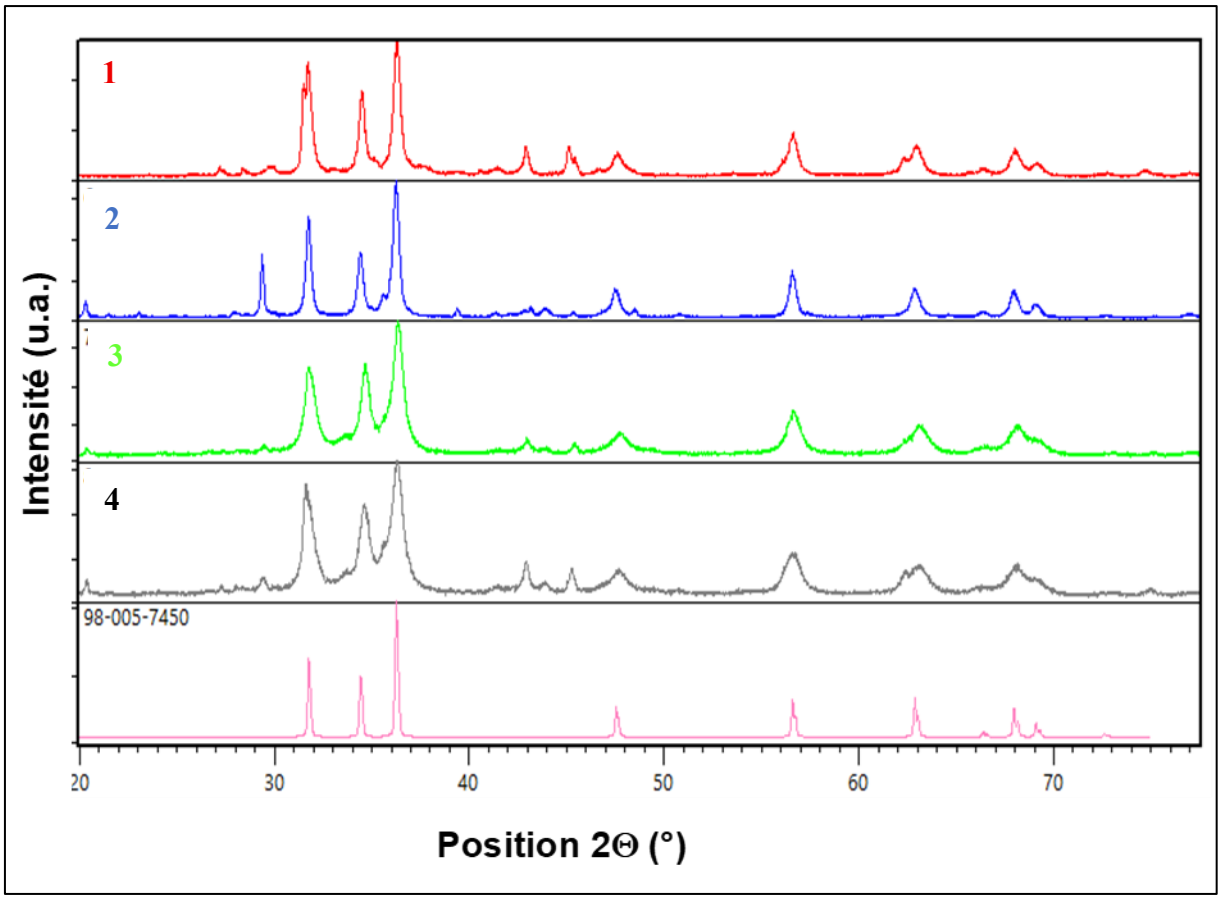

Figure IV.3. XRD patterns of the ZnO NPs's via green chemistry (1-Atriplex, 2-Urtica, 3-Horsetail and 4-Mixture) and ZnO.

All samples display characteristic diffraction peaks corresponding to the **hexagonal wurtzite** structure of zinc oxide, indexed according to ICSD reference 98-005-7450. The XRD patterns show peaks in the 2θ range of 20° to 70°, with the most intense reflections observed at 2θ = 31.7°, 34.4°, 36.2°, 47.5°, 56.6°, 62.8°, and 68.0°. These sharp peaks are assigned to the (100), (002), (101),

(102), (110), (103), and (112) crystallographic planes of the hexagonal wurtzite ZnO phase. The detailed diffraction patterns for each sample are presented in Figure IV.4.

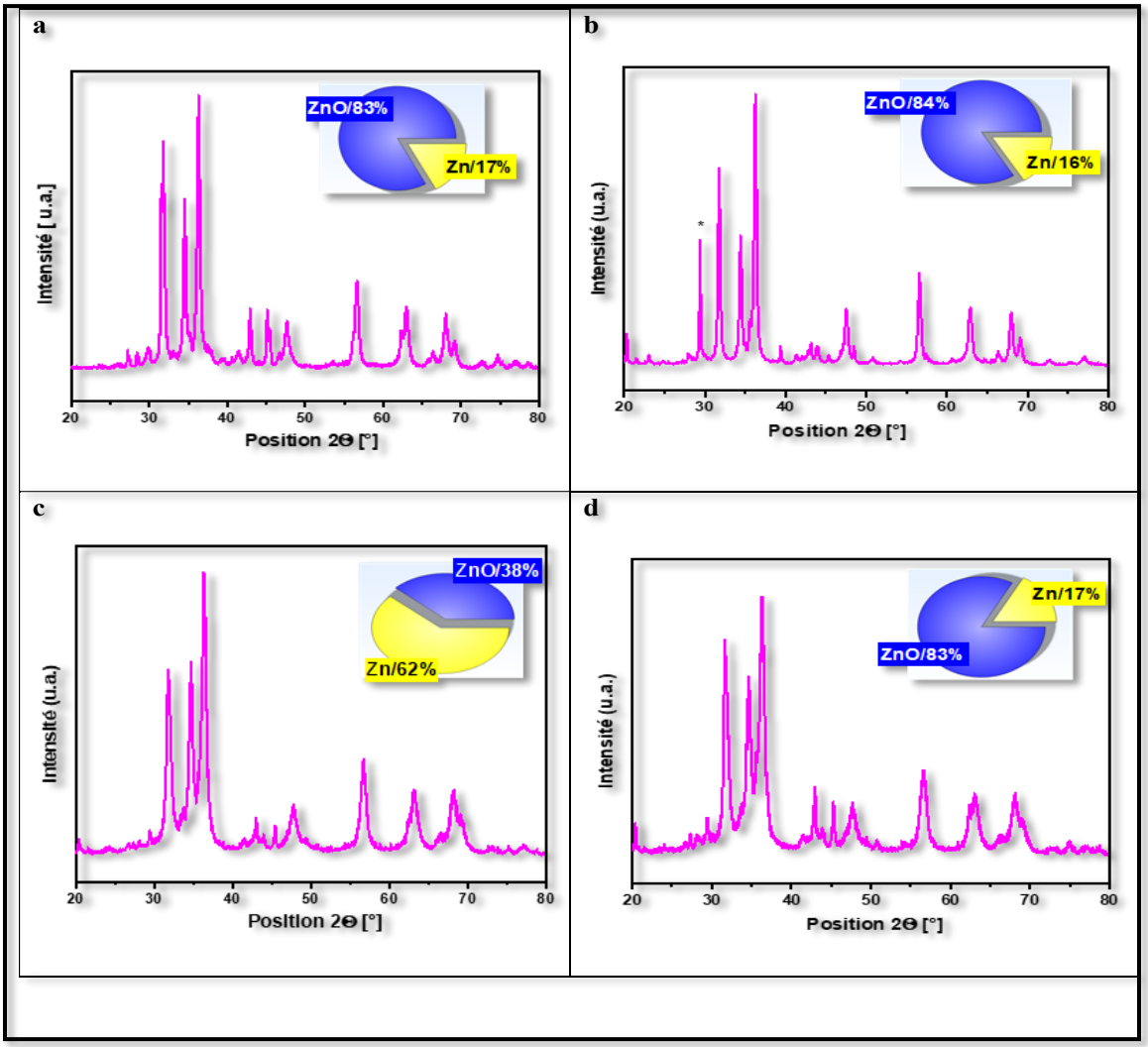

Figure.IV.4. (XRD) patterns overlaid with a pie chart illustrating the phase composition of the samples (a-Atriplex ZnO NPs; b-Urtica ZnO NPs; c-Horsetail ZnO NPs; d-Mixture ZnO NPs).

Each subfigure includes a pie chart showing the relative composition of ZnO and metallic Zn:

- **Atriplex (ZnO 83% / Zn 17%):** The XRD pattern exhibits intense and well-defined peaks, indicating high crystallinity of the nanoparticles. This can be attributed to the richness of the Atriplex extract in phenolic acids and flavonoids, which are known for their strong reducing and stabilizing properties.

- **Urtica (ZnO 84% / Zn 16%):** The Urtica extract yields a similar diffraction pattern with even higher peak intensities, also reflecting high crystallinity. This is likely due to the abundance of phenolic compounds in Urtica, which contribute effective reducing and stabilizing action during synthesis.
- **Horsetail (ZnO 38% / Zn 62%):** The spectrum obtained with the Horsetail extract displays broader peaks, suggesting lower crystallinity and potentially smaller crystallite size or increased amorphous content. The high proportion of metallic Zn indicates incomplete oxidation, resulting in a lower yield of ZnO.
- **Mixture of Extracts (ZnO 83% / Zn 17%):** The mixture of plant extracts produces an XRD pattern similar to those of Atriplex and Urtica, with sharp peaks and a predominant ZnO phase (over 80%). This suggests that combining extracts does not significantly alter the crystalline quality or phase composition compared to the individual extracts of Atriplex and Urtica.

These results demonstrate that synthesizing ZnO nanoparticles using different plant extracts provides valuable comparative insights into how phytochemical composition affects the synthesis process, crystallinity, and phase purity of ZnO nanoparticles. Notably, the use of Atriplex, Urtica, and the mixture of all three extracts consistently yields predominantly ZnO nanoparticles, with a ZnO content exceeding 80%. In contrast, the horsetail extract leads to incomplete oxidation, resulting in a much higher proportion of metallic Zn (62%) and a lower ZnO content (38%).

On the other hand, the average crystallite size was estimated by applying the Scherrer equation to the (011) diffraction peak observed around $2\theta \approx 36°$. This method is based on analyzing the full width at half maximum (FWHM) of the diffraction peak, which is influenced by crystallite dimensions and internal lattice strain. The Scherrer equation used is as follows:

$$\mathbf{D = (K \times \lambda) / (\beta \times \cos\theta)}$$

where:

- K is the shape factor, typically taken as 0.9
- λ is the wavelength of Cu Kα radiation (λ=1.5406 A˚)

- β is the full width at half maximum (FWHM) in radians
- θ is the Bragg angle (half of the 2θ value)

The table below presents the results calculated from the diffraction peaks around 2θ≈36°, corresponding to the (011) plane according to the ICSD reference card No. 98-005-7450 for ZnO.

Table IV.2. Structural properties and phase identification of Green-Synthesized ZnO Nanoparticles (1-4) by X-ray Diffraction

	Pos. [°2Th.]	d-spacing [Å]	Height [cts]	FWHM Left [°2Th.]	Crystallite Size [nm]	Micro Strain [%]
1	36,3114	2,47412	2504,23	0,2755	35,15013	0,351936
2	36,2604	2,47748	3275,23	0,1968	50,58415	0,244887
3	36,3785	2,46971	1631,06	0,3936	24,26512	0,508901
4	36,3595	2,47096	1360,35	0,3936	24,26379	0,509186

These findings clearly demonstrate that the synthesis parameters, most notably the choice of plant extract, play a crucial role in determining the crystalline structure, crystallite size, and degree of internal strain within the synthesized ZnO nanoparticles. Notably, the sample exhibiting a diffraction peak at **36.2604 °** (Urtica ZnO NPs) displays superior crystallographic properties, indicative of enhanced crystallinity and lower lattice strain. Such characteristics are highly advantageous for advanced applications where high structural order is critical, including photocatalysis, chemical sensing, and optoelectronic devices. This underscores the importance of optimizing synthesis conditions to tailor the structural attributes of ZnO nanoparticles for targeted functional performance.

IV.1.3. Optical characterization by UV-Visible Analysis

The optical absorption properties of nanomaterials are critically influenced by factors such as bandgap energy, oxygen vacancies, defects/impurities, and surface structure. The UV–visible spectroscopy serves as a powerful analytical tool for characterizing size- and shape-controlled nanoparticles in aqueous colloidal suspensions, as these parameters directly correlate with spectral features.

To estimate the optical bandgap of the synthesized nanoparticles, UV–visible spectroscopy (200 nm-800 nm) was performed. Zinc oxide nanoparticles (ZnO NPs) display a strong absorption band around 352 nm (λ_{max} for almost all the synthesized nanoparticles) in their UV-Vis spectra (Figure IV.5), which is significantly blue-shifted compared to bulk ZnO that typically absorbs at about 367 nm (corresponding to a band gap of ~3.37 eV). The optical band gap of the synthesized ZnO nanoparticles was determined to be **3.52 eV**, calculated using the formula: $Eg = 1240/\lambda_{max}$, where λ_{max} (in nm) corresponds to the maximum absorption wavelength in the UV-Vis spectrum [7, 8]. This value was consistent with the reported literature values of 3.52 eV for nanocrystalline ZnO particles synthesized [9], and 3.45 eV for the *Ocimum tenuiflorum* leaf extract mediated synthesis [10].

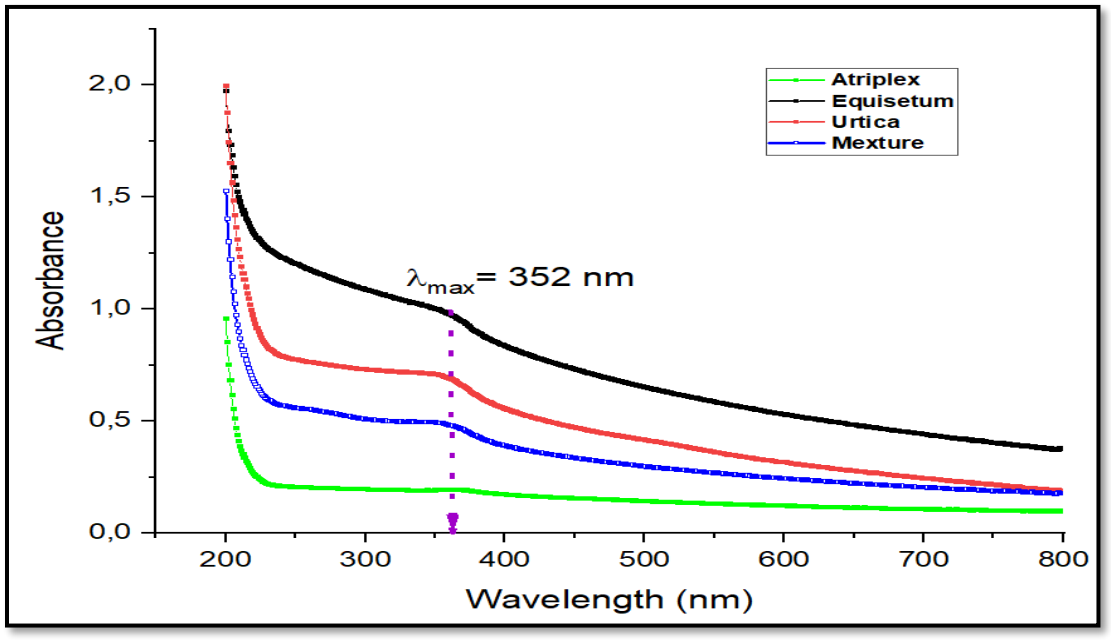

Figure.IV.5. UV-Vis Absorption Spectra of ZnO Nanoparticles synthesized using different plant extracts.

This blue shift is a hallmark of the quantum confinement effect, which occurs when the particle size approaches or falls below the exciton Bohr radius. Moreover, the energy separation between the highest occupied molecular orbital (HOMO) and the lowest unoccupied molecular orbital (LUMO) increases as particle size decreases, leading to a larger band gap and a shift of the absorption edge to shorter wavelengths (higher energies) [11]. This enhanced band gap enables ZnO nanoparticles to absorb higher-energy photons in the UV and near-UV regions of sunlight, efficiently generating electron-hole pairs critical for driving photocatalytic reactions.

IV.2. Photocatalytic ZnO NPs application

The photocatalytic degradation efficiency of ZnO nanoparticles was evaluated using rhodamine B (Rh B) dye under sunlight irradiation. **Figure IV.6** displays the temporal UV-Vis spectra of Rh B, illustrating the progressive decrease in its characteristic absorption peak at 554 nm. After 180 minutes of exposure, the absorbance intensity declined significantly across all samples: **Atriplex** (from 1.12 to 0.60), **Horsetail** (from 1.05 to 0.05), **Urtica** (from 1.18 to 0.28) and **Mixture** (from 1.00 to 0.02).

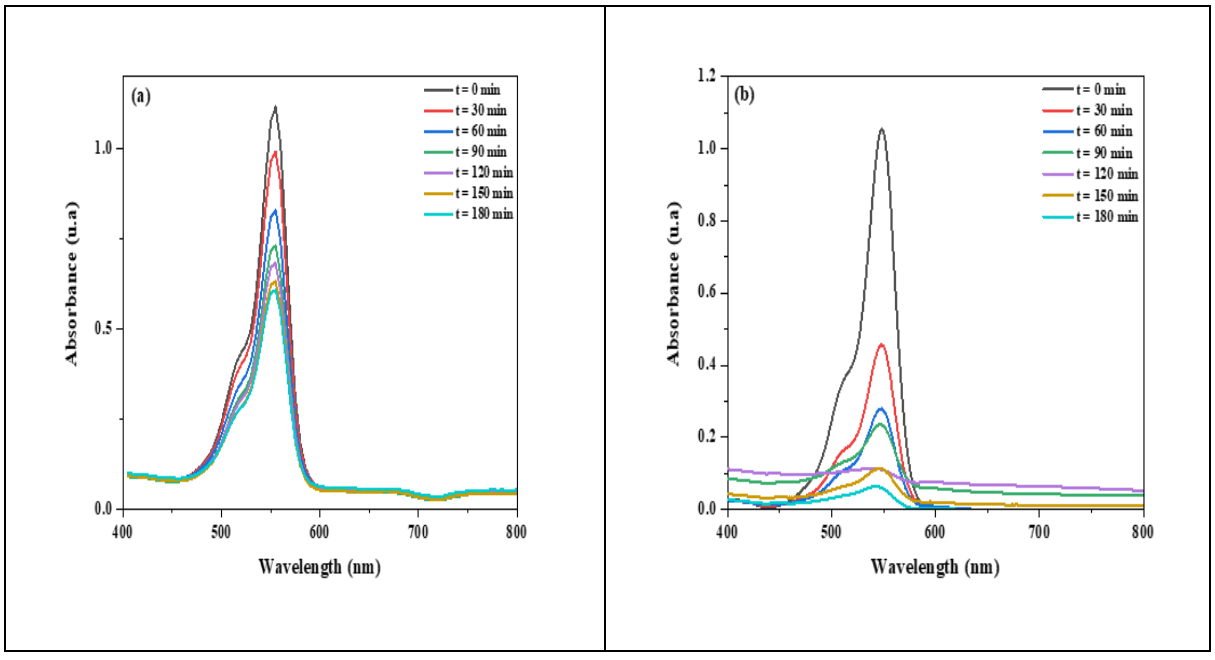

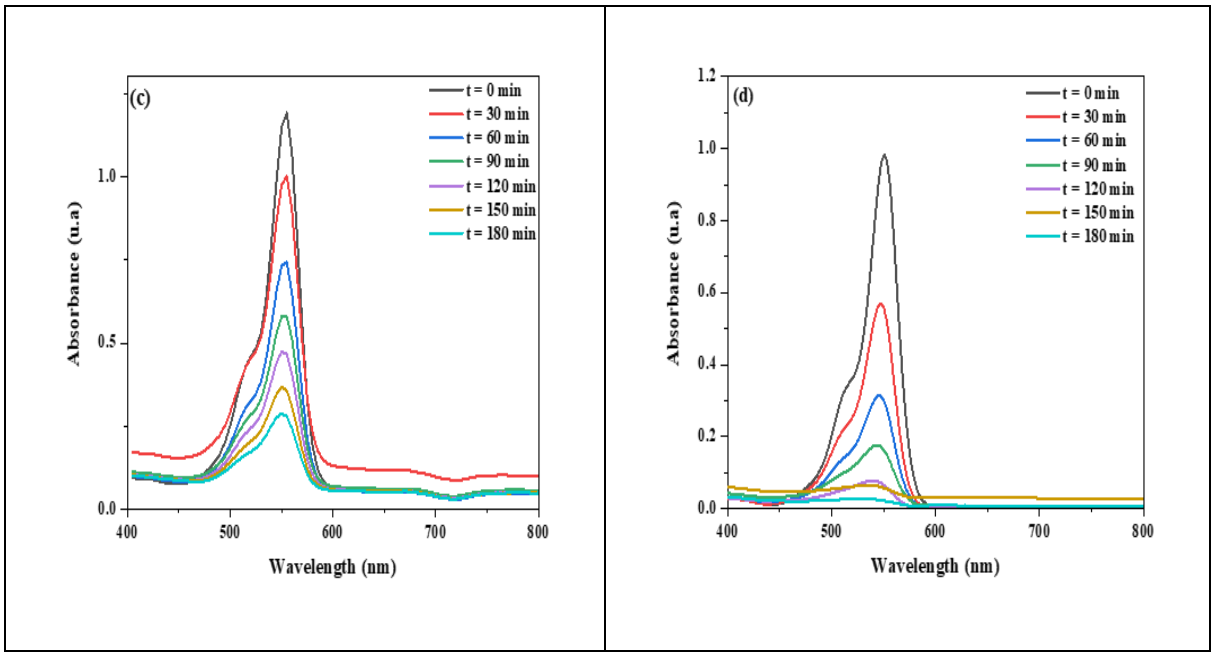

Figure.IV.6. Evolution of the absorption spectra of the RhB solution in the presence of the catalysts: (a) Atriplex, (b) Horsetail, (c) Urtica, (d) Mixture

The progression of Rh B dye photodegradation, catalyzed by ZnO particles as a function of sun light irradiation time, is depicted in (**Figure.IV.7)**. The data indicate a steady increase in dye degradation efficiency with prolonged exposure to sun light. The degradation efficacy of Rh B dye reached 57.26% (Atriplex), 94.32% (Horsetail), 76.52% (Urtica), and 97.87% (Mixture), after 180 min of sun light exposure. The rapid decline in peak intensity highlights the strong photocatalytic activity of ZnO NPs, attributed to the generation of reactive oxygen species (ROS) by photogenerated charge carriers under sun light. These results align with recent studies (Khumphon, J. et *al.*, 2025) reporting >90% Rh B degradation using defect-engineered ZnO nanostructures within comparable timeframes [12].

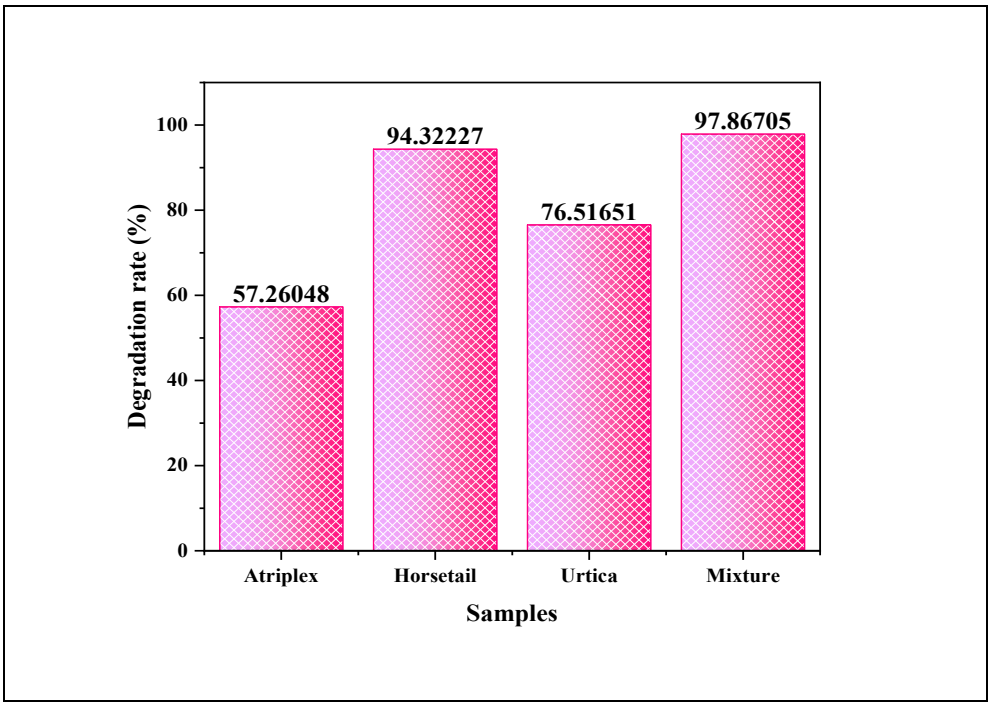

Figure.IV.7. Photocatalytic efficiency of RhB degradation by catalysts

The study concludes that green synthesis using a plant mixture is superior to individual plant sources in photodegrading RhB dye under the given conditions, likely due to complementary phytochemicals aiding better nanoparticle properties. Indeed, phytochemical capping agents in horsetail and mixture extracts may enhance dye adsorption via electrostatic interactions or hydrogen bonding, compensating for lower crystallinity. Surface hydroxyl groups (-OH) from plant extracts also improve dye adsorption and radical generation. However, further characterization such as BET and SEM analysis is needed to better describe the influence of structural morphology and defect properties on photocatalytic activity.

References

[1] Theophil Anand, G.; Renuka, D.; Ramesh, R.; Anandaraj, R.; John Sundaram, S.; Ramalingam, G.; Magdalane, C.M.; Bashir, A.K.H.; Maaza, M.; Kaviyarasu, K. Green synthesis of ZnO nanoparticle using Prunus dulcis (Almond Gum) for antimicrobial and supercapacitor applications. Surfaces and Interfaces 17 (2019)100376. https://doi.org/10.1016/j.surfin.2019.100376

[2] Fahad A. Alharthi, Abdulaziz Ali Alghamdi 1, Asma A. Alothman, Zainab M. Almarhoon, Munairah F. Alsulaiman and Nabil Al-Zaqri. Green Synthesis of ZnO Nanostructures Using Salvadora Persica Leaf Extract: Applications for Photocatalytic Degradation of Methylene Blue Dye. Crystals 2020**.**

[3] Smith, B.C. The Carbonyl Group, Part V: Carboxylates—Coming Clean. Spectroscopy 2018, 33, 20–23.

[4] Boyatzis, S.C.; Fragkos-Livanios, L.; Giannoulaki, M.; and Filopoulou, A. Infrared spectroscopy reveals the reactivity of fatty acids on copper surfaces and its implications for cultural heritage objects. Heritage Science (2023) 11:196. https://doi.org/10.1186/s40494-023-01023-1

[5] Ngoc Duong, T.B.; Pham, P.Q.; Tran, A.T.; Bui, D.T.; Thanh Pham, A.T.; Thi Nguyen, T.C.; Thuy Nguyen, L.H.; Thi Ung, T.D.; Hoang, N.V. and Kim Pham, N. Correlation between organic residuals of green synthesized nanoparticles and resistive switching behavior. RSC Adv., 2024, 14, 36340-36350, https://doi.org/10.1039/D4RA04381B

[6] Iqbal, J.; Abbasi, B.A.; Yaseen, T.; Zahra, S.A.; Shahbaz, A.; Shah, S.A.; Siraj Uddin, Ma, X.; Raouf, B.; Kanwal, S.; Amin, W.; Mahmood, T.; El-Serehy, H.A.; Ahmad, P. Green synthesis of zinc oxide nanoparticles using *Elaeagnus angustifolia* L leaf extracts and their multiple in vitro biological applications. Scientific Reports, Article number: 20988 (2021).

[7] https://instanano.com/all/characterization/uv-vis/band-gap/

[8] Balcha, A.; Yadav, O.P.; Dey, T. Photocatalytic degradation of methylene blue dye by zinc oxide nanoparticles obtained from precipitation and sol-gel methods, Environ.Sci. Pollut. Res. 23 (24) (2016) 25485–25493.

[9] Prakoso, S.P.; Saleh, R. Synthesis and Spectroscopic Characterization of Undoped Nanocrytalline ZnO Particles Prepared by Co-Precipitation, Materials Sciences and Applications, 2012, 3, 530-537. http://dx.doi.org/10.4236/msa.2012.38075

[10] Dayakar, T.; K. Venkateswara Rao, Bikshalu, K.; Rajendar, V.; Park, S.H. Novel synthesis and structural analysis of zinc oxide nanoparticles for the non-enzymatic glucose biosensor, Mater. Sci. Eng. C 75 (2017) 1472–1479.

[11] Ganvir, H.V.; Jonathan, B.; Kumar, K. S.; Raju, V. P.; Prabhakaran, K.; Prajwal, H. N. Validation of Size of Semiconductor Nano Material: Effect on Size and Shape, Communications on Applied Nonlinear Analysis. Vol 32 No. 2 (2025).

[12] Khumphon, J.; Ahmed, R.; Imboon, T.; Giri, J.; Chattham, N.; Mohammad, F.; Kityakarn, S.; Gowri, M. V and Thongmee, S. Boosting Photocatalytic Activity in Rhodamine B Degradation Using Cu-Doped ZnO Nanoflakes, ACS Omega 2025, 10, 9337−9350. https://doi.org/10.1021/acsomega.4c10034

CONCLUSION

Zinc oxide nanoparticles (ZnO NPs) are promising multifunctional materials due to their unique optical, electrical, and catalytic properties, as well as their safety and biocompatibility. In this study, ZnO NPs were successfully synthesized via a green, cost-effective, and environmentally friendly method using aqueous extracts of *Urtica dioica*, *Atriplex halimus*, and *Equisetum arvense* as both reducing and stabilizing agents. The bioactive compounds present in these plant extracts, such as phenolics, and flavonoids, facilitated the efficient formation and stabilization of the nanoparticles.

Comprehensive characterization by X-ray diffraction (XRD), UV-visible spectroscopy, and Fourier-transform infrared spectroscopy (FTIR) confirmed the successful synthesis of crystalline ZnO nanoparticles with a hexagonal wurtzite structure for all samples: Atriplex, Urtica, Horsetail, and the mixture. XRD analysis revealed that the average crystallite sizes varied among the samples: Urtica-derived ZnO NPs exhibited the largest crystallite size (about 50.6 nm), followed by Atriplex (35.2 nm), while Horsetail and mixture-derived ZnO NPs had smaller sizes (approximately 24.3 nm). All samples showed well-resolved diffraction peaks corresponding to the hexagonal ZnO phase, indicating good crystallinity, though the Horsetail and mixture samples displayed broader peaks, suggesting higher microstrain and defect density.

UV-Vis spectroscopy showed that the absorption edges for all ZnO nanoparticles were in the UV region, with calculated band gap energies of 3.52 eV. This consistent band gap across all samples highlights the need for robust UV characterization techniques (e.g., Tauc plots, diffuse reflectance spectroscopy) to further differentiate the optical behavior of ZnO NPs synthesized from different plant extracts.

FTIR analysis further confirmed the presence of phytochemical capping agents on the surface of all ZnO nanoparticles. Characteristic bands for O–H, C=O, and C–O functional groups were observed, indicating the successful incorporation of bioactive compounds from each plant extract onto the nanoparticle surfaces. The presence of these surface groups is likely to enhance the stability and dispersibility of the ZnO NPs and may also contribute to their photocatalytic activity.

The study demonstrates a time-dependent decrease in RhB concentration under sun light irradiation, confirming effective photodegradation mediated by ZnO nanoparticles. The mixture's superior performance likely stems from complementary phytochemicals (e.g., polyphenols, flavonoids) that enhance nanoparticle properties by improving charge carrier separation via surface passivation, increasing dye adsorption through electrostatic interactions or hydrogen bonding with surface hydroxyl (-OH) groups and by broadening light absorption via defect states.

Overall, these results highlight that the choice of plant extract in green synthesis critically influences the resultant ZnO nanoparticles' structural, optical, and surface characteristics. Specifically, the Mixture ZnO NPs demonstrate an advantageous combination of small crystallite size, a moderate band gap, and a rich surface chemistry. Consequently, this study strongly suggests that these Mixture ZnO NPs are promising candidates for use as effective photocatalysts in the removal of dyes from wastewater, offering a sustainable and efficient treatment approach.

ABSTRACT

This study presents a green, cost-effective synthesis of zinc oxide nanoparticles (ZnO NPs) using aqueous extracts of *Atriplex halimus*, *Urtica dioica*, *Equisetum arvense* (horsetail), and their mixture as both reducing and stabilizing agents. Comprehensive characterization by X-ray diffraction (XRD), UV-visible spectroscopy (UV-Vis), and Fourier-transform infrared spectroscopy (FTIR) confirmed the successful formation of crystalline ZnO NPs with a hexagonal wurtzite structure.

Photocatalytic activity was evaluated through the degradation of rhodamine B dye under sunlight. Remarkably, ZnO NPs synthesized using horsetail extract and the mixture of all three extracts demonstrated superior photocatalytic efficiencies, achieving up to 97% dye removal within 180 minutes.

Keywords: Green synthesis, zinc oxide nanoparticles, plant extracts, *Urtica dioica, Atriplex halimus, Equisetum arvense*, Photocatalysis, Rhodamine B.

ملخص

تقدم هذه الدراسة تخليقًا صديقًا للبيئة وفعّالًا من حيث التكلفة لجسيمات أكسيد الزنك النانوية باستخدام مستخلصات مائية من نبات القراص، ذيل الحصان القطف وخليطها كعوامل اختزال وتثبيت. اكد التوصيف الشامل باستخدام حيود الأشعة السينية، ومطيافية الأشعة فوق البنفسجية المرئية، ومطيافية الأشعة تحت الحمراء بتحويل فوربيه، التكوين الناجح لجسيمات نانوية بلورية من أكسيد الزنك مع بنية وورتزيت سداسية.

تم تقييم النشاط الضوئي التحفيزي من خلال تحلل صبغة رودامين ب تحت أشعة الشمس .ومن اللافت للنظر أن جسيمات أكسيد الزنك النانوية المُصنّعة باستخدام مستخلص ذيل الحصان، وقد أظهر خليط المستخلصات الثلاثة كفاءة ضوئية فائقة، حيث بلغت نسبة إزالة الصبغة 97% خلال 180 دقيقة

الكلمات المفتاحية: التخليق الاخضر، جسيمات أكسيد الزنك النانوية، المستخلصات النباتية، نبات القراص، ذيل الحصان الحقلي نبات القطف، التحفيز الضوئي، رودامين ب.

République Algérienne Démocratique et Populaire
Ministère de l'Enseignement Supérieur et de la Recherche Scientifique
Université Med Khider Biskra

Faculté des Sciences Exactes
Département des Sciences de la Matière
Filière de Chimie

الجمهورية الجزائرية الديموقراطية الشعبية
وزارة التعليم العالي و البحث العلمي
جامعة محمد خيضر بسكرة

كلية العلوم الدقيقة
قسم علوم المادة
شعبة الكيمياء

تصريح شرفي

خاص بالالتزام بقواعد النزاهة العلمية لإنجاز بحث

(ملحق القرار 1082 المؤرخ في 2021/12/27)

أنا المعضي أسفله،

السيد(ة):.....بوزيد.....مونة.....

الصفة: طالب سنة ثانية ماستر كيمياء تخصص:.....كيمياء.صيدلانية.

الحامل(ة) لبطاقة التعريف الوطنية رقم: 211355637 الصادرة بتاريخ: 25/02/12

المسجل بكلية: .....العلوم.الدقيقة.....قسم: .....علوم.المادة..... والمكلف

بانجاز أعمال بحث : مذكرة ماستر في الكيمياء

عنوانها: Green Synthesis, Characterization and Photocatalytic dye degradation activity of Nanoparticles (ZnO)

أصرح بشرفي أني ألتزم بمراعاة المعايير العلمية والمنهجية ومعايير الأخلاقيات المهنية والنزاهة الاكاديمية المطلوبة في انجاز البحث المذكور أعلاه وفق ما ينص عليه القرار رقم 1082 المؤرخ في 2021/12/27 المحدد للقواعد المتعلقة بالوقاية من السرقة العلمية ومكافحتها.

التاريخ: 2021/05/25

إمضاء المعني بالأمر